Ore Geology Reviews 57 (2014) 247–263

Contents lists available at ScienceDirect

Ore Geology Reviews

journal homepage: www.elsevier.com/locate/oregeorev

Spatio-temporal distribution and tectonic settings of the major iron deposits in China: An overview

Zhaochong Zhang [a,*], Tong Hou [a], M. Santosh [a,b], Houmin Li [c], Jianwei Li [d], Zuoheng Zhang [c], Xieyan Song [e], Meng Wang [a]

[a] State Key Laboratory of Geological Process and Mineral Resources, China University of Geosciences, Beijing, 100083, China
[b] Division of Interdisciplinary Science, Kochi University, Kochi 780-8520, Japan
[c] MLR Key laboratory of Metallogeny and Mineral Assessment, Institute of Mineral Resources, Chinese Academy of Geological Sciences, Beijing 100037, China
[d] State Key Laboratory of Geological Process and Mineral Resources, China University of Geosciences, Wuhan, 430074, China
[e] State Key Laboratory of Ore Deposit Geochemistry, Institute of Geochemistry, Chinese Academy of Sciences, 46th Guanshui Road, Guiyang, China

ARTICLE INFO

Article history:
Received 30 April 2013
Received in revised form 29 August 2013
Accepted 29 August 2013
Available online 5 September 2013

Keywords:
Iron deposits
Tectonic settings
Geodynamic control
Genetic features
China

ABSTRACT

China has a rich reserve of iron ores and hosts most of the major types of iron deposits recognized worldwide. However, among these, the banded iron formation (BIF), skarn, apatite–magnetite, volcanic-hosted, sedimentary hematite and magmatic Ti–Fe–(V) deposits constitute the most economically important types. High-grade iron ores (>50% Fe) are relatively rare, and are mostly represented by the skarn-type. Most of the BIF deposits formed in the Neoarchean, with a peak at ~2.5 Ga, and are mainly distributed in the North China Craton. The majority of these is associated with volcanic rocks, and therefore belongs to the Algoma-type. The superior-type BIF deposits formed during the Paleoproterozoic occur subordinately (ca. 25%), and are related mainly to rifts (or passive continental margins). In addition, minor Superior-type BIF deposits have also been recognized. The skarn iron deposits are widely distributed in China, especially in the uplifted areas of eastern China, and form several large iron ore clusters. These ore deposits are genetically associated with intermediate, intermediate-felsic and felsic intrusions with a peak age of formation at ca. 130 Ma. They display common characteristics including alteration and nature of mineralization. The apatite–magnetite deposits occurring in the Ningwu and Luzong Cretaceous terrigenous volcanic basins along the Middle–Lower Yangtze River Valley, are spatially and temporally associated with dioritic subvolcanic intrusions. The ores in this type are characterized by magnetite and apatite. The volcanic-hosted iron deposits are associated with submarine volcanic-sedimentary sequences, and are widely distributed in the orogenic belts of western China, including Western Tianshan, Eastern Tianshan, Beishan, Altay, Kaladawan area in the eastern part of the Altyn Tagh Mountain and southwestern margin of South China Block. These deposits show a considerable age range, from Proterozoic to Mesozoic, but with more than 70% were formed in the Paleozoic, especially during the Late Paleozoic. The metallogenesis in these deposits can be correlated to the space–time evolution of the submarine volcanism, and their relationship to volcanic lithofacies variation, such as central, proximal and distal environments of ore formation. The sedimentary hematite deposits are widespread in China, among which the "Xuanlong-type" in the North China Craton and the "Ningxiang-type" in the South China Block are the most economically important. All these deposits formed during transgressions in a shallow-marine environment. Magmatic Ti–Fe–(V) deposits are dominantly distributed in the Panxi area in Sichuan province and Chengde area in Hebei province. They are dominated low-grade disseminated ores, and unlike the other types of iron deposits, associated sulfide deposits are absent, with magnetite, titanomagnetite and ilmenite as the dominant ore minerals. In the Panxi area in the central Emeishan large igneous province along the western margin of South China Block, the ores are hosted in the ca. 260 Ma mafic layered intrusions, whereas the ores in the Chengde area are associated with the Mesoproterozoic anorthosite complex. The distinct spatio-temporal characteristics of the various iron deposits in China correlate with the multiple tectono-magmatic events associated with the prolonged geological history of the region involving accretion, assembly and rifting.

1. Introduction

In a recent classification scheme (Dill, 2010), iron deposits have been grouped into four types: magmatic iron deposits, structure-related iron deposits, sedimentary iron deposits and metamorphic deposits or band

* Corresponding author. Tel.: +86 10 82322195; fax: +86 10 82323419.
E-mail address: zczhang@cugb.edu.cn (Z. Zhang).

0169-1368/$ – see front matter
http://dx.doi.org/10.1016/j.oregeorev.2013.08.021

iron formation (BIF) deposits. Each of these iron deposits has been further divided into two or more sub-types. Among these types, the magmatic iron deposits have been further divided into five sub-types: 1) magmatic Ti–Fe–(V) deposits related to mafic intrusions (high Ti), 2) apatite–magnetite deposits (low Ti), 3) apatite–magnetite deposits related to alkaline–carbonatite complex, 4) contact metasomatic Fe deposits (Fe skarn) and 5) volcanic-hosted Fe unmetamorphosed deposits. The BIF deposits have been traditionally divided into Algoma- and Superior-types. Thus, a total of 14 sub-types have been classified by Dill (2010). Among all these types of iron deposits, BIF deposits are the most important iron resource, and account for >85% and >90% of high-grade iron ore resources (>50% Fe) and total iron resources, respectively (Zhang et al., 2012a). They are hosted in Archean greenstone belts located within Archean and Proterozoic cratons in association with granitoids and gneisses (Basta et al., 2011; Konhauser et al., 2007; Pickard, 2003).

In China, all the 14 sub-types of iron deposits worldwide have been recognized, although BIF, contact metasomatic (skarn), apatite–magnetite (low Ti), volcanic-hosted, sedimentary hematite, magmatic Ti–Fe–(V) deposits (high Ti) are the most economically important six types. Although BIFs make up 58% of the total iron reserves in China, in contrast to the global iron resources, the high-grade iron ores (>50% Fe) in China occupy only ~1%, and are predominantly from skarn-type (H.M. Li et al., 2012). This peculiar feature is related to the unique situation of extensive reactivation and destruction of the North China Craton through multiple tectonic cycles, and the prolonged interaction among the Central-Asian, Circum-Pacific and Tethys-Himalayan geodynamic systems (Zhao and Zhai, 2013).

Although several studies have addressed the characteristics and genesis of the different types of iron deposits in China, a compilation of their detailed information is not available in the international literatures. In this paper, therefore, we attempt to provide updated information on the six major types of iron deposits in China, with emphasis on the link between their spatio-temporal distribution and geodynamic processes in order to better understand the regional genetic controls on these deposits.

2. An outline of the tectonics of China

The tectonic architecture of China continent is defined by three Precambrian continental cratons or blocks: the North China Craton (NCC), the South China Block (SCB, Cathaysian Block + Yangtze Craton) and the Tarim craton surrounded by a series of Phanerozoic fold belts incorporating several micro-continental blocks (Fig. 1a) (Wang et al., 2013; Zhai and Santosh, 2011, 2013; Zhang and Zheng, 2013; Zhao and Zhai, 2013; Zheng et al., 2013, and references therein). The Precambrian tectonic framework has been overprinted by differential reactivation and destruction, as well as accretion in response to the prolonged subduction of the Pacific and Indian plates and related geodynamic processes (e.g., Guo et al., 2013; Yang et al., 2013). Ren et al. (1999) proposed that the tectonic configuration of China is dominated by three global tectonic systems, the Central-Asian, the Circum-Pacific and the Tethys–Himalaya systems (Fig. 1a). The Mesozoic–Cenozoic Circum-Pacific tectonic belt in eastern China was produced by the subduction of Pacific/Izanagi plate beneath the Eurasian continent, whereas the Tethys–Himalaya system in southwestern China led to the indentation of the Indian continent into Eurasia. The Central-Asian tectonic system in northern China consists of a series of broadly E-W-trending fold belts, which, from north to south, include the Altay–Ergune, Junggar, and Tianshan–Hing'an Range (Fig. 1b). These fold belts occur along the margins of the Siberian, Tarim and the North China Cratons (Xiao et al., 2013).

3. Iron resources in China

China has one of the richest reserves in the world after Brazil, Australia, Ukraine and Russia. More than 2000 iron deposits have been discovered and explored until now, including 12 super-large iron deposits (>1000 Mt of ores), 100 large iron deposits (100–1000 Mt of ores), 380 middle iron deposits (10–100 Mt of ores) and more than 1500 small iron deposits (<100 Mt of ores). However, most of these are low-grade ores (<50% Fe, Fig. 2a), and the high-grade iron ores only account for ~1% of the total iron ore resources.

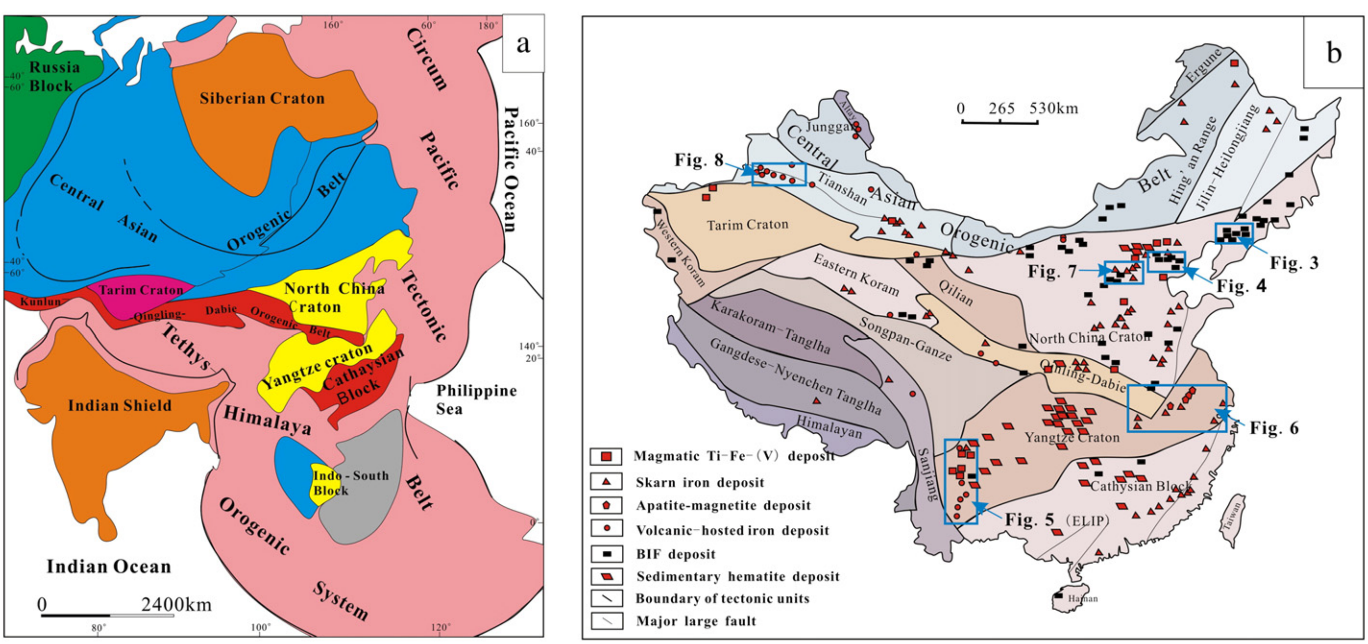

Fig. 1. a) Sketch tectonic map of China continent and adjacent regions (modified from Ren et al., 1999); b) distribution of the major types of iron deposits in China (modified from Zhao et al., 2004). The locations of Figs. 3–8 are shown. Small iron deposits and other types of iron deposits are not shown in the map.

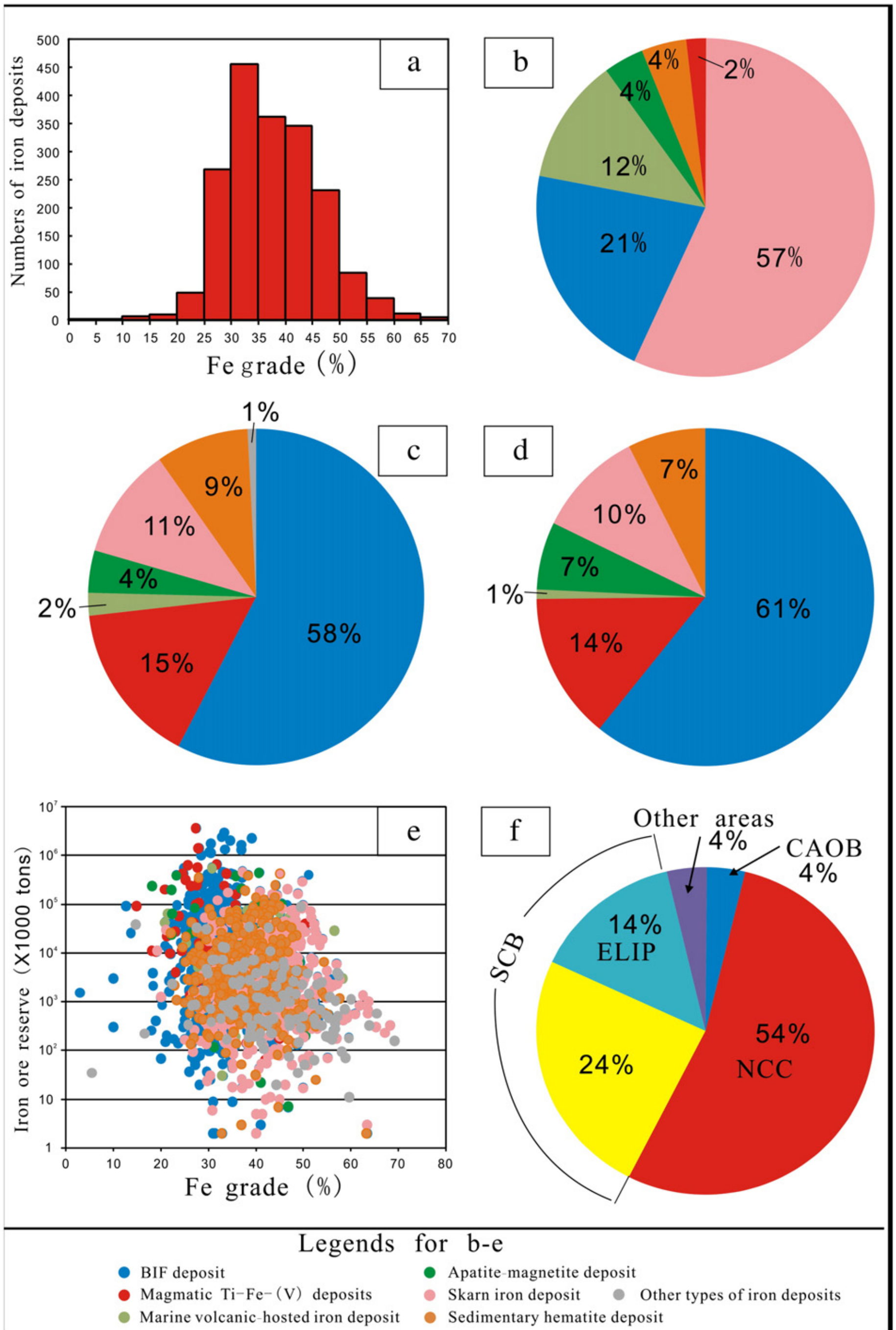

Fig. 2. Statistics of iron resources in China (Data sources: Ministry of Land and Resources, unpublished data): a) Histogram of Fe grades of deposits in China; b) high-grade iron resources of different types of iron deposits in China; c) total iron ore resources of different types of iron deposits in China; d) statistics of large iron deposits in China; e) grade versus tonnage diagram of different types of iron deposits in China; f) iron ore resources of major tectonic units in China (Emeishan large igneous province belong to a part of South China block because it is located in the western margin of South China block).

Among the high-grade iron ores, about 57% belong to the skarn iron deposits (Fig. 2b). Like in other countries, BIF deposits are the most important iron ore resources in China (Fig. 2c) and contain most of the large iron deposits of the entire country (Fig. 2d), although they account for 21% of the high-grade iron ores (Fig. 2b). However, the iron ore reserves do not correlate with the iron grades (Fig. 2e).

Spatially, the iron deposits are irregularly distributed across China. More than 50% of the iron ores in China are concentrated in the Liaoning, Sichuan and Hebei provinces. The remaining iron resources are mainly in Beijing, Shanxi, Inner Mongolia, Shandong, Henan, Hubei, Yunnan, Anhui provinces and in Xinjiang (Fig. 1b). When the iron ore resource data are examined in a tectonic framework, more than 92% of iron ore resources are located in the NCC and the SCB including those associated with the Emeishan large igneous province (ELIP). Those in the ELIP account for 14.5% of the total iron resources (Fig. 2f). The iron deposits in the Central Asian Orogenic Belt (CAOB) and other tectonic units account for less than 4%.

4. Major types and characteristics of iron deposits in China

In this section, we summarize the general features of the six important types of iron deposits in China: BIF, skarn, apatite–magnetite, volcanic-hosted, submarine volcanic-hosted, sedimentary hematite and magmatic Ti–Fe–(V) deposits. More specific descriptions of the individual iron deposits are presented in the other papers of this special issue.

4.1. BIF deposits

The BIF iron deposits or BIFs are dominantly distributed in the NCC, with minor BIFs in southern margin of the SCB, Qinling, Qilian and Kunlun orogenic belts (Fig. 1b). The Anshan–Benxi in Liaoning province, Eastern Hebei–Miyun in Beijing, Wutai and Lüliang in Shanxi province and Middle Inner Mongolia are the most important BIF ore clusters (Fig. 1b).

Based on the available isotopic age data, the formation of Precambrian BIFs in China can be divided into six episodes (Shen, 2012; Zhao et al., 2004) as follows: 1) 3.5–3.2 Ga, represented by the Xingshan and Huangboyu iron deposits in eastern Hebei province hosted in the Fuping Group. The associated rocks have been dated at 3470 ± 107 Ma (Jahn et al., 1987), 3495 ± 15 Ma (Qiao et al., 1987) and 3352 ± 50 Ma (Shen et al., 2004) by Sm–Nd isochronic method are only possibly representatives. 2) 3.2–2.8 Ga, represented by the Shuichang large iron deposit and other medium–small scale iron deposits in eastern Hebei province hosted in the Qianxi Group. 3) 2.8–2.5 Ga, represents the peak time for the formation of BIFs. The host strata include Neoarchean Anshan, Zunhua, Taishan, Huoqiu, Dengfeng and Luanhe Groups, represented by the major large and superlarge iron deposits such as Gongchangling in Liaoning and Sijiaying in eastern Hebei province (Shen, 2012). 4) 2.56–2.45 Ga, the host strata are Wutai Group and Lüliang Group in Shanxi province (Shen, 1998), and the representative iron deposits are Yuanjiacun in Shanxi province and Jining in Shandong province. 5) 1.8–1.7 Ga, the host strata is Jingtieshan Group in Gansu province and is represented by the large Jingtieshan iron deposit in Gansu province. 6) 0.80–0.54Ga, the iron deposits of this age are predominantly distributed in the southeastern margin of the SCB, including the Xinyu iron deposit in Jiangxi province and Shilu iron deposit in Hainan province, and represent the unique great high-grade iron deposit in China, and are also the largest high-grade hematite ore deposit in Asia (Xu et al., 2013, in this issue).

Like BIFs in other countries (Gross, 1965), the Precambrian BIFs in China can be divided into the Algoma-type associated with volcanic rocks, and the Superior-type stratabound in sedimentary sequences (Zhai and Santosh, 2011, 2013). However, the Algoma-type BIFs are the dominant source for iron in China in contrast to the Superior-type BIFs providing the major source in other main iron-produced countries of the world such as Brazil, Australia, Russia and Ukraine. The Algoma-type BIFs were predominantly formed in Neoarchean, whereas the Superior-type were generated in Paleoproterozoic (James, 1983; Trendall, 2002). An exception is the BIF in the Jining Group which has been considered to be a Superior-type, and from where W. Wang et al. (2010) obtained an age of 2.56 ± 0.02 Ga.

Based on the major host rocks of the BIFs, the following five include five rock associations can be recognized (Zhang et al., 2012b): 1) amphibolites (or hornblende plagioclase gneiss) and magnetite quartzite association; 2) amphibolites, biotite leptynite, mica quartz schist, and magnetite quartzite association; 3) biotite leptynite (or biotite quartz gneiss) and magnetite quartzite association; 4) biotite leptynite, sericite chlorite schist, biotite quartz schist and magnetite quartzite association; and 5) amphibolites (gneiss), marble and magnetite quartzite association. The protolith of the host rocks are of three types: 1) mafic volcanic rocks (tholeiitic)-dominated with pelitic–arenaceous rocks; 2) sedimentary rocks intercalated with volcanic rocks; and 3) tuffaceous rocks-bearing sedimentary succession. All of these lithologies have experienced variable-grades of metamorphism, from lower-greenschist facies to granulite facies. In general, the metamorphic grades are closely related to the formation of BIFs. The Paleoarchean and Mesoarchean BIFs generally experienced granulite-facies metamorphism, and the Neoarchean BIFs have undergone amphibolite-facies metamorphism. The post-Paleoproterozoic BIFs metamorphism is only up to the lower greenschist facies.

The BIF deposits contain several layers of ores. The orebodies are stratiform, lenticular, up to 200–300 m thick, hundreds to thousands of meters long, and extend to hundreds to a few thousands of meters in depth. The orebodies show evidence for multiple and intense deformation. Magnetite is the dominant ore mineral in almost all the BIF deposits, but minor deposits also contain considerable amounts of hematite and martite with minor siderite. Quartz, chlorite, cummingtonite, almandine and carbonate are the most common gangue minerals. The most common ores are low grade, with 20–40% total Fe and 40–50% SiO_2. High-grade ores are subordinate, and no more than 1% of the total ore reserves.

The high-grade ores are usually enclosed within the thick-layer low-grade orebodies, and controlled by faults and folds, especially in the axis of syncline. These high-grade ores were possibly formed by three mechanisms (H.M. Li et al., 2012; Shen, 2012) as follows: The first category is primary deposit in origin as exemplified by the Waitoushan deposit in Benxi area of Liaoning province and the Sijiaying deposit in eastern Hebei province. The relative high-grade ores occur within the low-grade thick-layer ores without any distinct boundary, and are conformable with their country rocks. The second type could be formed by later structure-hydrothermal superimposition, and represent the most common type of high-grade ores with the, following features: 1) most of ores are controlled by faults and folds, and especially concentrated in the axis of folds; 2) all high-grade ores are hosted in the low-grade ores or magnetite quartzite, and the low-grade ores have generally been replaced by the high-grade ores; 3) magnetite is the dominant ore mineral as against hematite as the principal ore mineral in other cratons worldwide; 4) intense hydrothermal and migmatization are widespread in the high-grade ores; 5) many orebodies tend to become larger with depth. The third type is related to the weathering of the ancient crust. Although this type is the most widespread in other cratons, it is rather rare in China, and represented only by the Tieguken deposit in Henan province, Zhangzhuang deposit in Anhui province and Xianshan in Liaoning province belong to this type (H.M. Li et al., 2012; Zhao et al., 2004). All the orebodies of this type are small, and are not economically important.

The Shilu large high-grade iron deposit in Hainan province has been recently interpreted as BIF type (Xu et al., 2013, in this issue). The deposit is hosted in the Neoproterozoic Shilu Group, comprising a suite of green-schist facies metamorphosed marine clastic–carbonate succession of siltstone, mudstone and carbonate. Unlike the other BIF deposits in China, one of the notably distinctive features for the Shilu ores is the ore minerals dominated by hematite, locally with minor magnetite (<1%). The iron ores generally show banded and massive structures with lepidoblastic, cryptocrystalline or microcrystalline textures. Although the origin of the Shilu iron deposit is still debated, it has been commonly considered to be the product of a multi-stage evolution, with several overprinting events after its formation that might have significantly modified the ores. Based on field and petrographic observation in combination with isotopic age data, Xu et al. (2013) proposed four-stage metallogenic model: (1) deposition of the BIF-type ore source horizons between ca. 830 and 960 Ma; (2) formation of a metamorphic sedimentary-type ore deposit during ca. 830–360 Ma; (3) refinement of the deposit through tectonics attending the deformation at ca. 250 to 210 Ma; and (4) superposed mineralization stage by magma-related hydrothermal fluids at ca. 130 to 90 Ma. Xu et al. (2013) concluded that the latter three stages of remarkable superimposition and modification have contributed to the formation of an unusually large hematite-dominated iron deposit.

4.2. Skarn iron deposits

Skarn or contact metasomatic iron deposits occur in the country rocks as well as in the skarn mineralization at the contact zone between pluton and carbonate as lens-, layer-like, veined or irregular shapes. This type of iron deposit is the most widespread in China. Except in the Tianjin, Chongqing, Guizhou and Taiwan provinces, these deposits have been discovered in all other provinces, and show concentric distribution in the middle of NCC, SCB, Qinling orogenic belt, Tianshan orogenic belt and Tibet Plateau (Fig. 1b).

Based on the lithology of the ore-related intrusions, the iron deposits can be divided into three groups as follows.

1) Iron deposits associated with intermediate intrusions. This type occurs mainly in the depression domains along the margins of the uplifted region in the NCC. The ore-related intrusions are mainly Cretaceous dioritic and monzonitic rocks, which were emplaced into the Middle Ordovician carbonate-dominant strata containing some evaporites (Cai et al., 1987). Albite alteration is quite common, and sodalite alteration has also been locally recognized. Magnetite is the dominant ore mineral with some martite and Co-bearing pyrite. The unique feature of this category is the association of Co.
2) Iron deposits associated with intermediate-felsic intrusions. These deposits occur in the uplifted areas of the SCB, such as the Daye area in the Middle–Lower Yangtze River Valley (MLYRV, Li et al., 2009). The ore-related intrusions are Late Jurassic–Early Cretaceous diorite, quartz diorite, granodiorite and monzogranite complex. The wall rocks are mainly Triassic limestone or dolomitic limestone. Alkali alteration such as albitization and sodalitization is common. K-feldspar alteration can also be locally recognized. Magnetite is also a dominant ore mineral with some martite, pyrite, and chalcopyrite, commonly coupled with Fe, Cu, Co and Au paragenesis.
3) Iron deposits associated with felsic intrusions. These deposits occur mainly in zones of depression along the continental margin such as the Great Hinganling in northeast China, Yanshan in Hebei province, East Qinling mountains and along the coast of southeast China. The ore-related intrusions are granite and granodiorite. In general, the granite intrudes tuff and muddy or sandy rocks interbedded with carbonates, whereas granodiorite intrudes the thick-layer dolomite or dolomitic limestone. The ages of the intrusions in different tectonic domains are different. Those in eastern China were formed in Mesozoic, those in northwestern and northeastern China are Late Paleozoic and Triassic, and those in the western margin of the SCB are Neoproterozoic. Four types of ore mineral assemblages have been recognized: marmatite–magnetite, cassiterite–magnetite, molybdenite–magnetite and molybdenite–chalcopyrite–sphalerite–magnetite. In some cases, Fe, Cu, Pb, Zn, W, Sn, Bi and Mo mineralization have been identified in the same deposit, e.g., the Cuihongshan iron deposit in Northeastern China (He et al., 2010). Additionally, there are many tin, boron, beryllium, and fluorine-bearing minerals in some deposits, although they are only minor. Alkali alteration is common, especially potassic alteration, including K-feldspar, biotite and sericite alteration, in contrast to the albite alteration in other types.

The accompanying elements in the skarn iron deposits depend upon the lithology of the ore-related intrusions. From intermediate intrusion (diorite and monzonite) to intermediate-felsic complex (diorite, quartz diorite, granodiorite), and to felsic intrusion (granodiorite and granite), the corresponding accompanying elements are Co (Cu, Au), to Cu, Pb, Zn, and then to Cu, Pb, Zn, W, Sn, Mo, Bi. The accompanying elements are also related to nature of the wall rocks.

Skarns can be subdivided into magnesian and calcic skarn according to the dominant skarn minerals. Usually, calcic skarn is the dominant variety, and only few iron deposits identified in recent studies show the occurrence of magnesian iron skarns such as the Tonglushan skarn Cu–Fe deposits in Hubei province (e.g., Zhao et al., 2012), Dading skarn Fe polymetallic deposit in Guangdong (e.g., Zheng et al., 2009), those in the Taershan region in south Shanxi province (e.g., Huang et al., 2006) and Cuihongshan skarn Fe polymetallic deposit in Heilongjiang province (e.g., He et al., 2010). The formation of calcic skarn is related to the limestone wall-rocks, whereas the formation of magnesian skarn can be ascribed to dolomite wall-rocks. The calcic skarn minerals contain diopside–hedenbergite series, grossular–andradite series, wollastonite, scapolite and vesuvian garnet. In contrast, diopside, forsterite, spinel, phlogopite, serpentine, humite, and talc are typical of magnesian skarns. In addition, except for magnetite, magnesian magnetite or magnesioferrite locally occur in magnesian skarns. Some other minerals, such as calcite, are also present in almost of the skarns.

The skarn iron deposits are small to medium in scale with only few large iron deposits (e.g., Daye iron deposit). The orebodies are tens to hundreds of meters, up to thousands of meters in length, several to tens of meters in thickness, and tens to hundreds of meters in depth. Most of the ores possess massive structure with disseminated and breccia structures locally. The replacement texture is the most common. The grade of ores ranges from 30 to 70%.

4.3. Apatite–magnetite deposits

Apatite–magnetite Fe deposits, also known as Kiruna-type deposits, occur in a number of localities in the world, ranging in age from Proterozoic to Cenozoic, and are associated with intermediate volcanic rocks or sub-volcanic intrusions (Nyström and Henriquez, 1994). This type of iron deposit is known as porphyry-type iron deposit (Ningwu Research Group, 1978; Zhang, 1986) or terrestrial volcanic type (H.M. Li et al., 2012; Zhao et al., 2004). Almost all such deposits are present in the Ningwu and Luzong Cretaceous terrigenous volcanic basins along MLYRV. So far, there are 35 known deposits in the NNE-trending Ningwu basin and 11 in the NE-trending Luzong basin (Mao et al., 2011). The Meishan in Jiangsu province, Gushan, Washan, Taocun, Heshangqiao, Baixiangshan, Luohe, Nihe and Longqiao in Anhui province have large iron deposits.

The iron metallogeny in this case is genetically related to the Early Cretaceous dioritic subvolcanic intrusions belonging to shoshonite series. The iron orebodies are developed along the contact zones between the dioritic subvolcanic intrusions and volcano-sedimentary rocks. Thus, these iron orebodies can be hosted in the Early Cretaceous volcanic rocks that are derived from the common sources with the subvolcanic intrusion (Zhou et al., 2011), or occur in the apical zones of the dioritic subvolcanic intrusions.

Five types of ores have been identified: massive, stockwork-disseminated, brecciated, banded and skeleton ores. The most common styles are stockwork-disseminated which make up 90% volume of the ores. Almost all massive ores and part of the brecciated ores have an average Fe grade of ~45 wt.%. In addition, the massive ores contain 0.1–1.34% P, 0.03–8% S and 0.1–0.3% V. Both stockwork-disseminated and massive ores spatially occupy the apical zones of the dioritic volcanic intrusions. The hydrothermal veins are superimposed either on the major orebodies or along the fractures of surrounding volcanic rocks. Although the different styles of ores have been considered to be caused by different mechanisms, there is a general consensus that they are genetically related, and formed from a co-magmatic-hydrothermal system (e.g., Chang et al., 1991; Hou et al., 2010, 2011; J.J. Yu et al., 2011; Mao et al., 2011; Ningwu Research Group, 1978; Tang et al., 1998; Zhai et al., 1992, 1996; Zhang, 1986; Zhao et al., 2004; Zhou et al., 2010, 2011).

Ore minerals are magnetite, hematite, pyrite and rare chalcopyrite with major gangue minerals represented by albite, diopside, actinolite, apatite, epidote, anhydrite, chlorite and sericite. In some deposits, such as the Nihe iron deposit, karstenite is abundant.

The hematite/magnetite ratio shows a general increases towards the surface (Ningwu Research Group, 1978). The mineralization and alteration processes can be divided into three stages: early anhydrous silicate alteration, middle retrograde alteration and late argillic–carbonate alteration. The anhydrous silicate alteration is dominated by pyroxene and garnet with extensive albitization. The retrograde alteration zones are composed of hydrous silicates, such as actinolite, chlorite, epidote and phlogopite. Magnetite is a dominant mineral in the retrograde alteration stage, overprinting the early alteration stage. The late argillic–carbonate alteration is dominated by quartz, clays, carbonates, anhydrite and alunite. Some of the magnetites have been altered by martite at this stage. Spatially, the alteration pattern consists of three zones (J.J. Yu et al., 2011 and reference therein): (1) an upper leucocratic zone, consisting predominantly of albitite or diopside-bearing albitite with minor actinolite, titanite, apatite, and magnetite; (2) a middle melanocratic zone, composed of diopside, apatite, and magnetite; almost all economic iron ores are concentrated in these zones; and (3) a lower leucocratic zone, characterized by extensive argillic, kaolinite, silica, carbonate and pyrite alteration associated locally with some small pyrite orebodies.

4.4. Volcanic-hosted iron deposits

The volcanic-hosted iron deposits, or commonly named as submarine volcanic iron deposits by Chinese geologists (e.g., H.M. Li et al., 2012; Jiang, 1983; Jiang and Wang, 2005; Zhao et al., 2004), is one of the most important iron deposits hosting high-grade of iron ores. They have been recognized to be widely present in orogenic belts, mostly located in western China, including Western Tianshan, Eastern Tianshan, Beishan, Altay, Kaladawan area at eastern part of the Altyn Tagh Mountain and southwestern margin of SCB. The Awulale belt in the western Tianshan, which includes several large iron deposits and many medium–small iron deposits with a total ore reserve of >1000 million tons of ores at average grade of 40% (up to >60%), is of potential significance for China in recent exploration.

The volcanic-hosted iron deposits in China show a considerable age range in formation, from Paleoproterozoic (such as the Dahongshan large iron deposit in Yunnan province) to Mesozoic. However, more than 70% of these formed in the Paleozoic, especially in Late Paleozoic (such as the Awulale belt in the Tianshan orogenic belt and the south margin of Altay orogenic belt).

The iron deposits are commonly associated with submarine volcanic-sedimentary sequences, both lavas and pyroclastic-sedimentary rocks. The ore-related volcanic rocks exhibit a compositional spectra from intermediate-basic to intermediate-acid rocks and the volcaniclastic equivalents, but most are intermediate-basic. However, the iron deposits associated with the different rock units have distinct geological characteristics. The orebodies associated with pyroclastic-sedimentary rocks generally occur in stratiform, lenticular and lensoidal shapes, such as the Motuosala and Shikebutai iron deposits in the Awulale belt, western Tianshan, Xinjiang. The ores are characterized by banded hematite alternating with red jasper (red iron-bearing chert). Hematite is the dominant ore mineral with minor magnetite and/or rhodochrosite and hausmannite. The gangue minerals are quartz and barite with minor calcite, chlorite and sericite. Alteration is not common, with low-temperature alteration, e.g., chlorite, sericite, silica and calcite alteration. In contrast, the iron deposits associated with lavas occur as stratiform, lenticular and veined or complex veined shapes. The veined orebodies are controlled by faults, whereas the stratiform and lenticular orebodies, which are tens to hundreds of meters in thickness and hundreds to few thousands of meters in length, are dominantly controlled by stratigraphic horizons. Most of these orebodies have distinct boundaries with their wallrocks, and have massive structures, but some orebodies exhibit a zoning pattern with the high-grade massive ore in the center grading outward to disseminated ore, and have obscure boundaries with their wallrocks. Examples include the Paleoproterozoic Dahongshan iron deposits in Yunnan province. Extensive pervasive alteration around orebodies is widespread in all those iron deposits associated with volcanic rocks. The dominant alteration minerals are garnet, diopside, chlorite, epidosite, calcite, quartz, K-feldspar, albite, actinolite and sulfides, and the main ore mineral is magnetite. One of the most notable features for this type of iron deposit is that skarns are common in many of these such as the Beizhan and Chagangnuoer in West Tianshan, Yamansu in Eastern Tianshan, Mengku and Qiaoxiahala in Altay and Dahongshan in Yunnan province, developed in the contact zone between the orebodies and limestone rocks that are intercalated with felsic and intermediate volcanic magmas. However, unlike the classic skarns that are developed at the contact between pluton and carbonate rocks, no plutons are present near the skarns in the above iron deposits. The mineralization can be generally divided into three stages: 1) prograde stage: clinopyroxene + garnet ± albite ± scapolite; 2) retrograde stage: magnetite + amphibole ± scapolite + epidote + chlorite + quartz; and 3) sulfide stage: pyrite + chalcopyrite + pyrrhotite + chlorite + quartz + calcite. In addition, the Abagong iron deposit in Altay orogenic belt is characterized by abundant apatites associated with the ores. Two generations of apatite have been recognized, the first generation appears as a euhedral to subhedral mosaic with interstitial magnetite and fluorite, and the second generation is poikiloblastic apatite that overprints magnetite. Obviously, the Abagong iron deposit resembles Kiruna-style mineral systems (Chai et al., in this issue; Pirajno et al., 2011).

Although the origin of this type of iron deposit is controversial, they have been inferred to be directly or indirectly related to submarine volcanism, and possibly represent the different volcanic facies around the vent (Dong et al., 2011; Hou et al., in this issue). Those associated with pyroclastic-sedimentary rocks could represent the distal vent facies, whereas the stratiform and lenticular orebodies intercalated with lavas and pyroclastic rocks could be the proximal vent facies. The veined orebodies in lavas might have formed around the vent where faults and fissures are developed (Z. H. Zhang et al., 2012).

4.5. Sedimentary hematite iron deposits

Sedimentary hematite deposits occur widely in China (Fig. 1b). Based on the environment of deposition, they can be divided into continental and marine iron deposits. However, the continental iron deposits are economically insignificant, whereas the marine iron deposits are one of the most important types of iron deposits. They formed under favorable bathymetric and geodynamic conditions on shallow marine shelves or in epicontinental basins on stable cratons. They are controlled by facies but not necessarily time-related during transgressions in a shallow-marine environment.

The iron ores are associated with shales, sandstones and siltstones. In one iron deposit, there are generally 1–4 iron ore layers, each of which is relatively thin, mostly from tens of centimeters to several meters. Hematite and siderite are the most common ore minerals, and chamosites are present in some deposits. They usually display oolitic and massive structures with a minor brecciated category. In general, the hematite ores contain 30–55% Fe and 15–35% SiO_2, but Fe grades are negatively correlated with SiO_2. In addition, the ores also contain 0.02–0.2% S and 0.4–1.1% P. In comparison, the siderite ores grade from 25% to 40% Fe.

The most important sedimentary hematite deposits in China include the “Xuanlong” type and the “Ningxiang” type. The “Xuanlong” type of iron deposits with a total of 290 Mt of ore resources are distributed in the NCC (Fig. 1b). They are associated with the Mesoproterozoic Changcheng Group, consisting of a transgression sequence of clastic rocks, pelitic rocks and limestones. They generally include 1–4 layers of 0.5–3 m thick hematite ores and one layer of 0.35–0.4 thick siderite ore. In contrast, the “Ningxiang” type of iron deposits with a total of 3740 Mt of ore resources is widespread in the SCB (Fig. 1b). They are hosted in Middle–Upper Devonian strata composed dominantly of sandstone, siltstone and shale. The ore layers range from 1 to 6, although the thick and main layers are from 1 to 3.

Previous studies suggest that for both “Xuanlong” and “Ningxiang” types of iron deposits, the Fe was derived from iron-bearing formations in continents, and delivered by rivers into various basins and embayments in colloidal state. Microbial activity probably played a key role during Fe accumulation in the near-shore environments (e.g., H.M. Li et al., 2012).

4.6. Magmatic Ti–Fe–(V) deposits related to mafic intrusions

The magmatic Ti–Fe–(V) deposits are associated with and hosted within mafic–ultramafic intrusions. They are characterized by enrichment in V and Ti, distinctive from the other types of iron deposits. These iron deposits are dominantly distributed in the Panxi (Panzhihua–Xichang in Sichuan province) area and the Chengde area in Hebei province, with only minor and small-scale iron deposits occurring locally discovered in other areas (Fig. 1b). They have been confirmed to carry 10,000 million tons of ore reserve. However, ~95% of the ore reserves have been recognized in the Panxi area, making China a major Ti and V producer (Zhou et al., 2005 and references therein). These iron deposits have a notable general feature that low-grade of disseminated ores are dominant although high-grade of massive ores have been identified in some iron deposits such as the Panzhihua in the Panxi area (Arndt, 2013a, 2013b; Dong et al., 2013; Hou et al., 2012; Pang et al., 2013; Zhang et al., 2009) and Damiao in Chengde area (Li et al., in this issue; Zhao et al., 2009). Unlike other types of iron deposits, sulfide deposits are absent in this type, with magnetite, titanomagnetite and ilmenite as the dominant ore minerals.

The mineralization ages, or those of the ore-related mafic–ultramafic intrusions range from Mesoproterozoic to Mesozoic, but show a peak in Middle Permian (Panxi area) and Mesoproterozoic (Chengde area). According to rock association, they can be classified into two styles, one with gabbro-dominated layered intrusion and the other one with Proterozoic anorthosite complex. The first category is represented by those in the Panxi area, and the second one is represented by those in the Chengde area, Hebei province. The main characteristics of the two categories are described below.

Compared with those associated with Proterozoic anorthosite complex, the iron deposits associated with gabbro-dominated layered intrusion are more common. The ore-related intrusion comprises large layered mafic–ultramafic plutons with several up to 10 km in length and hundreds of meters to 1 km in width. The rock associations include olivine pyroxene–gabbro, gabbro–anorthosite, (olivine) gabbro–norite, gabbro–troctolite, gabbro–olivine pyroxene–wehrlite. In general, throughout the intrusion, the frequency of V–Ti–iron oxide layers decreases upwards. Mineral compositions also show regular upward variations. For example, forsterite (Fo) contents of olivine and anorthite (An) contents of plagioclase decrease upwards. The compositions of clinopyroxenes are less variable. Based on differences in internal structure and the extent of oxide mineralization, the plutons can be generally divided into four lithologic zones: a marginal zone at the base, followed successively upwards by a Ti–Fe–(V) oxide-bearing gabbro zone (lower zone), a layered gabbro zone with some oxide orebodies (middle zone), and leucogabbro zone (upper zone). The marginal zone is markedly heterogeneous, and consists of fine-grained hornblende-bearing gabbro intercalated with olivine gabbro. The Ti–Fe–(V) oxide ore-bearing gabbro zone is composed of layered melanogabbros with major Ti–Fe–(V) oxide layers (the ore bodies). The layered gabbro zone consists of layered gabbro occasionally interbedded with several thin Ti–Fe–(V) oxide layers, whereas the leucogabbro zone consists mainly of unmineralized leucogabbro. This zone lacks any V–Ti–Fe layers.

In contrast with the large mafic–ultramafic complexes elsewhere in the world, such as the Bushveld and Stillwater, where iron oxide bodies are hosted in the upper zone, the thick iron oxide orebodies in their counterparts in China occur mostly in the lower and middle zones, which, according to recent models, are correlated with the frequent replenishment of fractionated mafic magma (Song et al., 2013). In addition, in some iron deposits such as the Xinjie and Hongge iron deposits (e.g., Zhong and Zhu, 2006; Zhong et al., 2004), the platinum-group element orebodies have been identified in the lower zone consisting of ultramafic rocks. Additionally, not all ore-bearing mafic–ultramafic plutons are layered, but they have significant compositional variation, suggesting that the magmas have undergone high degree of differentiation. However, the massive ores are generally absent in these plutons.

The second type of iron deposits is associated with Proterozoic anorthosite complex, and is recognized only in the Chengde area in the NCC. The complex is exposed over ~120 km^2, and consists predominantly of anorthosite (~85–90%) with norite and mangerite as well as minor troctolite and hornblendite, all of which are cut by gabbroic and ferrodioritic dikes. Two types of anorthosites occur in this area, white and gray, with the white anorthosite as the dominant variety. In addition to plagioclase, titanomagnetite is also common in the gray anorthosite. Geochronological studies employing U–Pb zircon dating on mangerite has yielded an average of 1.74 ± 0.02 Ga for the emplacement of these rocks, correlated to Mesoproterozoic rifting in the NCC (Zhang et al., 2007).

The ore bodies in this category are of two types of ores: disseminated and massive ores. The disseminated ores are generally hosted in gabbro at the contact zone between gabbro and anorthosite, and have no distinct boundary with the gabbro. The main ore minerals are magnetite and titanomagnetite, and the gangue minerals include pyroxene, plagioclase, apatite and rutile. In contrast, the massive ores show sharp contact with anorthosite, and are hosted in the vertical fractures of the previously consolidated anorthosites or troctolite. They can be broadly divided into Fe–Ti oxide and Fe–Ti–P oxide types (nelsonite). The massive ores in the lower parts of ore bodies grade upward into Fe–Ti–P oxide-rich gabbro with increasing abundance of silicate minerals. The breccias of anorthosite can be commonly observed in the massive ores. The main ore minerals are titanomagnetite with minor ilmenite. Post-magmatic alteration has been recognized, and the alteration minerals include chlorite, zoisite and uralite, which are considered to be of hydrothermal origin (Li et al., in this issue).

5. Main iron ore clusters in China

As mentioned in a previous section, the iron deposits in China show heterogeneous distribution. In the following section we summarize the salient information on the distribution and regional characteristics of the six important iron ore clusters in China.

5.1. Anshan–Benxi iron ore cluster

The Anshan–Benxi iron cluster hosts the largest iron resource in China, including 16 large and super-large iron deposits such as the Qidashan, Dagushan, Donganshan, Yanqianshan, Nanfen, Waitoushan, Beitai and Gongchangling, and many medium–small iron deposits (Fig. 3). These deposits constitute an iron ore cluster extending E–W for 5 km and N–S for 60 km over an area of ~5000 km^2. All the deposits in this ore cluster belong to BIF deposits with a total reserve of 12.5 billion tons of iron ores, accounting for 24.2% of the total iron reserve of China (H.M. Li et al., 2012).

The ore cluster is located in the northeast margin of the NCC. The exposed strata belong predominantly to the Neoarchean Anshan Group, which has been divided into lower, middle and upper Anshan sub-groups.

From base upward, the Lower Anshan sub-group consists of Chengzitong Formation (Fm.) and Tongshicun Fm. The Chengzitong Fm. is composed of plagioclase/pyroxene amphibolite, biotite plagioclase amphibole leptynite, garnet amphibolite and elcogite intercalated with BIFs. The Tongshicun Fm. comprises biotite plagioclase leptynite and garnet plagioclase leptynite intercalated with BIFs. Both formations are more than 5000 m thick.

The middle Anshan sub-group can be divided into three formations from base upwards: the Shanchengzi, Yanlongshan and Dayugou formations. The Shanchengzi Fm. consists predominantly of plagioclase amphibolite intercalated with lens-like BIFs. The Yanlongshan Fm. is mainly composed of migmatitic biotite gneiss interbedded with

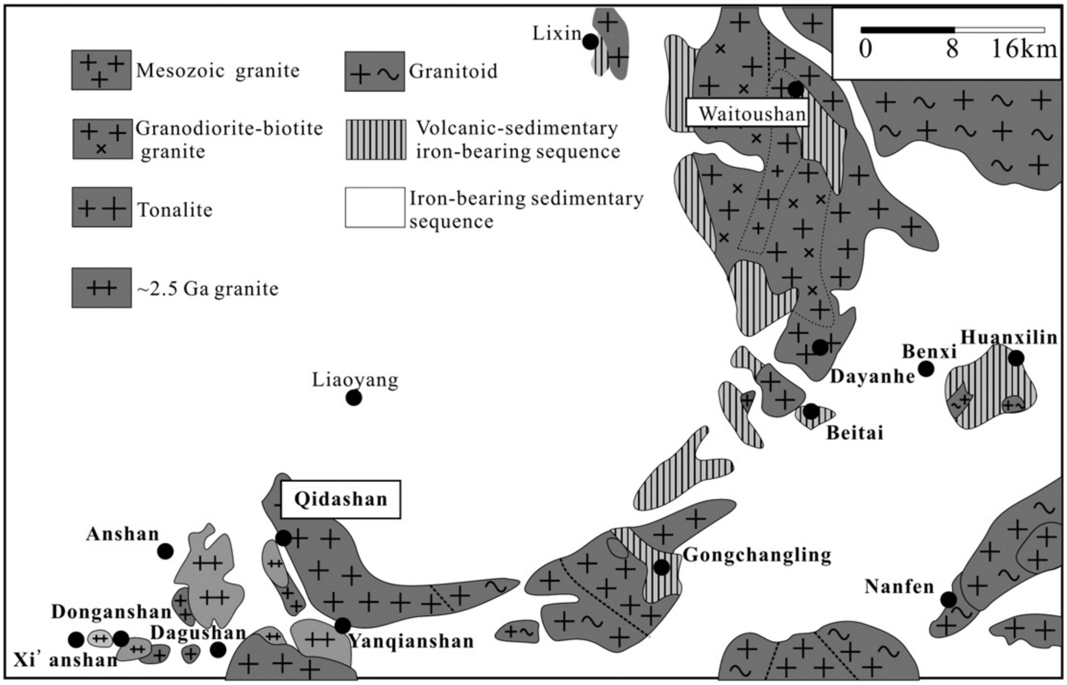

Fig. 3. Sketch geological map and distribution of the iron deposits in the Anshan–Benxi iron ore cluster, Liaoning province. After Shen (1998).

plagioclase amphibolite and mica quartz schist as well as two layers of BIFs, whereas the Dayugou Fm. which is the most widespread, comprises biotite leptynite intercalated with plagioclase amphibolite, mica quartz schist, two mica leptynite, two mica schist and garnet chlorite schist locally interbedded with several layers of BIFs.

Discordantly overlain by the Paleoproterozoic Liaohe Group, the upper Anshan sub-group consists of Yingtaoyuan Fm., composed of quartz chlorite schist, biotite leptynite and plagioclase amphibolite intercalated with a thick layer of BIF and locally with one or two minor layers of BIFs.

The protolith of the Anshan Group is considered to have formed at >2.8 Ga, followed by metamorphism at 2.65–2.5Ga (Zhao et al., 2004 and reference therein). However, recent SIMS U–Pb zircon dating on the amphibolite of the middle Anshan sub-group from the Waitoushan iron deposit yielded the age of 2.53 Ga (Dai et al., 2012), confirming a Neoarchean magmatic event.

Regionally, the orebodies have been identified from all the above three sub-groups of the Anshan Group, but they display somewhat different features. 1) The iron orebodies are hosted in the green schist to lower amphibolite facies metamorphic rocks of the upper sub-group. The protoliths of the host metamorphic rocks are sedimentary sequences. The iron deposits consist of a thick large layered orebody 100–300 m thick and several tens of kilometers long. One or two other small layered orebodies also occur such as those in the Donganshan, Xianshan, Qianshan and Yanqianshan deposits. All these iron deposits are large or super-large in scale. 2) The iron orebodies are hosted in the amphibolite facies metamorphic rocks of the middle sub-group. The protolith of the host metamorphic rocks is a suite of intermediate-basic to intermediate-acid volcanic rocks interlayered with sedimentary rocks. The iron deposits generally comprise many parallel layers of orebodies. Each ore layer is generally 20–60 m thick. The total thickness of all orebodies is up to ~160 m. These iron deposits are generally of large or medium scale, with a few in small ones. The typical examples are Gongchangling, Nanfen, Waitoushan and Xiaolingzi deposits. 3) The iron orebodies are hosted in the amphibolite to granulite facies metamorphic rocks of the lower sub-group. The protolith of the host metamorphic rocks is a suite of mafic volcanic rocks. The iron deposits also comprise many parallel layers of thinly-layered orebodies. Each ore layer is generally 10–20 m thick. The total thickness of all these orebodies is up to 20–40 m. These iron deposits are generally of small scale such as the Luobokan iron deposit.

In general, the BIF deposits in the Anshan–Benxi iron ore cluster are generally considered to be Algoma-type. However, some workers argued that those hosted in the green schist to lower amphibolite facies metamorphic rocks of the upper sub-group of the Anshan Group belong to Superior-type (e.g., Hou et al., 2007; Y.H. Li et al., 2010, 2012b).

5.2. Eastern Hebei iron ore cluster

The ore cluster is tectonically located in the northern margin of the NCC, and is the second largest iron ore cluster after the Anshan–Benxi iron ore cluster in China. The ore cluster includes several large-superlarge iron deposits (e.g., Xingshan, Sijiaying, Shuichang, Shirengou, Mengjiagou, Shachang, Zhalanzhangzi and Malanzhuang) as well as many medium-scale ones. All the deposits in the ore cluster belong to BIF-type with a total reserve of ~6.3 billion tons of iron ores, accounting for ~15% of the total iron reserve of China. It has been reported in Chinese literature that many new orebodies with a total of more than 1.4 billion tons of iron ores were discovered by exploration in recent years. In addition, many magnetic anomalies detected from geophysical investigations remain to be assessed.

The outcrop strata contain Archean metamorphic rocks, Proterozoic, Paleozoic and Mesozoic sedimentary rocks and Quaternary cover (Fig. 4). Igneous rocks in this region comprise granite, granodiorite, diorite, syenite, monzonite, pyroxenite, gabbro and minor mafic dykes. These magmatic suites were emplaced mainly in the Neoarchean and again in the Mesozoic.

BIFs are hosted in the Precambrian rocks, including Paleoarchean, Mesoarchean, Neoarchean and Paleoproterozoic strata (e.g., L.C. Zhang et al., 2012a; Wan et al., 2011; Zhang et al., 2011). The salient characteristics of the ore-bearing strata from early to late are outlined below.

The Paleoarchean Caozhuang Group exposed in the Qianxi area of Eastern Hebei province is composed of plagioclase amphibolite, amphibole plagioclase gneiss, garnet biotite plagioclase gneiss interlayered BIFs. The Xinshan iron deposit is a typical example. The ores consist of

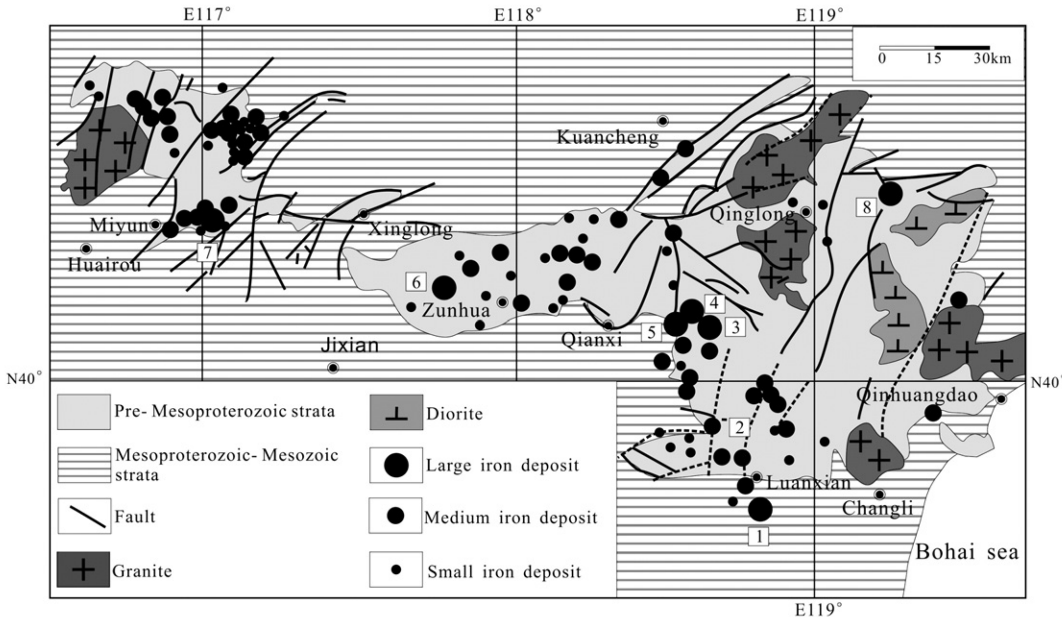

Fig. 4. Sketch geological map and distribution of the iron deposits from the eastern Hebei province to Miyun in Beijing. Important deposits: 1 — Sijiaing; 2 — Xingshan; 3 — Malanzhuang; 4 — Shuichang; 5 — Mengjiagou; 6 — Shirengou; 7 — Shachang; 8 — Zhalanzhangzi.
Modified from Zhao et al. (2004).

magnetite, in association with quartz and pyroxene with minor amphibole and chlorite.

The Mesoarchean Qianxi and Miyun Groups are exposed in the Qianxi region of Eastern Hebei province and Miqun region in northern Beijing and comprise pyroxene plagioclase gneisses, biotite plagioclase hypersthene gneiss and sillimanite garnet plagioclase gneiss interlayered with BIFs. The representative iron deposits are Shuichang, Mengjiagou in Qianan region and Shachang in Miyun. The ores consist of magnetite, together with quartz, hypersthene, diopside with variable amounts of amphibole, biotite, garnet and plagioclase as well as minor hematite, apatite, chlorite, talc and sulfides.

The Neoproterozoic strata in the Eastern Hebei province can be divided into three groups from bottom to top. 1) The Zunhua Group is composed of pyroxene plagioclase granulite, biotite plagioclase amphibole gneiss and plagioclase amphibolite interbeded BIFs. The iron deposits are represented by Shirengou and Longwan in the Eastern Hebei province. The ores contain magnetite, together with quartz, diopside and amphibole with variable amounts of plagioclase, hypersthene, actinolite and biotite as well as minor apatite, chlorite, carbonate and sulfides. 2) The Luanxian Group consists mainly of biotite amphibole gneiss and plagioclase amphibolite interbeded BIFs. The Sijiaying iron deposit in the Eastern Hebei province is hosted in this group. The principal ore is magnetite, together with quartz, actinolite and amphibole with variable amounts of hematite, plagioclase, talc, and biotite as well as minor apatite, chlorite, carbonate and sulfides. 3) The Shuangshanzi Group consists mainly of leptynite, biotite plagioclase amphibolite and garnet biotite schist interbeded with minor BIFs.

In the Miyun region, northeast Beijing, the Neoarchean strata is represented by the Zhangjiafeng Group, and is composed predominantly of biotite plagioclase gneiss, plagioclase amphibole schist and amphibolite interlayered BIFs, represented by Fengjiayu iron deposit in Miyun region. The ores contain magnetite, quartz, biotite and amphibole with variable amounts of plagioclase and garnet.

The Paleoproterozoic Zhuzhangzi Group exposed in Eastern Hebei consists mainly of mica schist, leptynite and minor plagioclase amphibolite interlayered BIFs, represented by the Zhazhangzi iron deposit. The ores contain magnetite, quartz, cummingtonite, tremolite and actinolite with minor biotite and garnet as well as rare hematite, apatite, carbonate and sulfides.

Most of the iron deposits in this region are hosted in the Neoarchean Zunhua Group and the Luanxian Group. Four types of protoliths of the host rocks can be identified: BIFs with volcanic rocks, BIFs with volcanic and minor sedimentary rocks, BIFs with volcano-sedimentary rocks and BIFs with dominantly sedimentary units and minor volcanic rocks. The older strata have experienced much higher degree of metamorphism and contain bigger grains of magnetite.

5.3. Xichang–Xinping iron ore cluster

The iron ore cluster is tectonically situated in the western margin of the SCB, extending from Xichang in Sichuan province to Xinping in Yunnan province, and controlled by a group of N–S-trending faults (Fig. 5). This cluster is the third largest one in China. The ore cluster includes several large–superlarge iron deposits such as the Hongge (4.572 billion tons of ore reserves), Panzhihua (1.333 billion tons of ore reserves), Baima (1.497 billion tons of ore reserves), Taihe (0.81 billion tons of ore reserves, Ma et al., 2003) and Dahongshan (0.5 billion tons of ore reserves) and many medium-scale iron deposits. A total reserve of ~10 billion tons of iron ores, which accounts for ~15% of the total reserve of China, has been explored.

The basement rocks in the ore cluster consist of the Archean to Paleoproterozoic granulite to amphibolite-facies metamorphic rocks which are known as the Kongling Complex that were dated at 2.95–2.9 Ga (Qiu et al., 2000), Meso- to Neoproterozoic low-grade metamorphic rocks of Kunyang and Huili Groups dated at ca. 1.0 Ga (Greentree et al., 2006; Sun et al., 2009) and Neoproterozoic Kangdian granitoids (ca. 800 Ma, Zhou et al., 2002) also occur in the region. The basement is overlain by a thick sequence (~9 km) of Cambrian to Mesozoic strata, in the absence of late Ordovician to Carboniferous strata owing to regional uplift and/or erosion. The pre-Permian strata are characterized by clastic and carbonate rocks. The Permian strata include carbonate-rich rocks and the Emeishan continental flood basalts. Triassic strata include both continental and marine sedimentary rocks, whereas Jurassic to Cretaceous strata are entirely continental.

Neoproterozoic arc granitic and mafic–ultramafic plutons occurred along the western and northern margin of the SCB, which have been correlated to subduction of Rodinian oceanic lithosphere toward the Yangtze craton during 760 to 860 Ma (Zhou et al., 2002). Middle

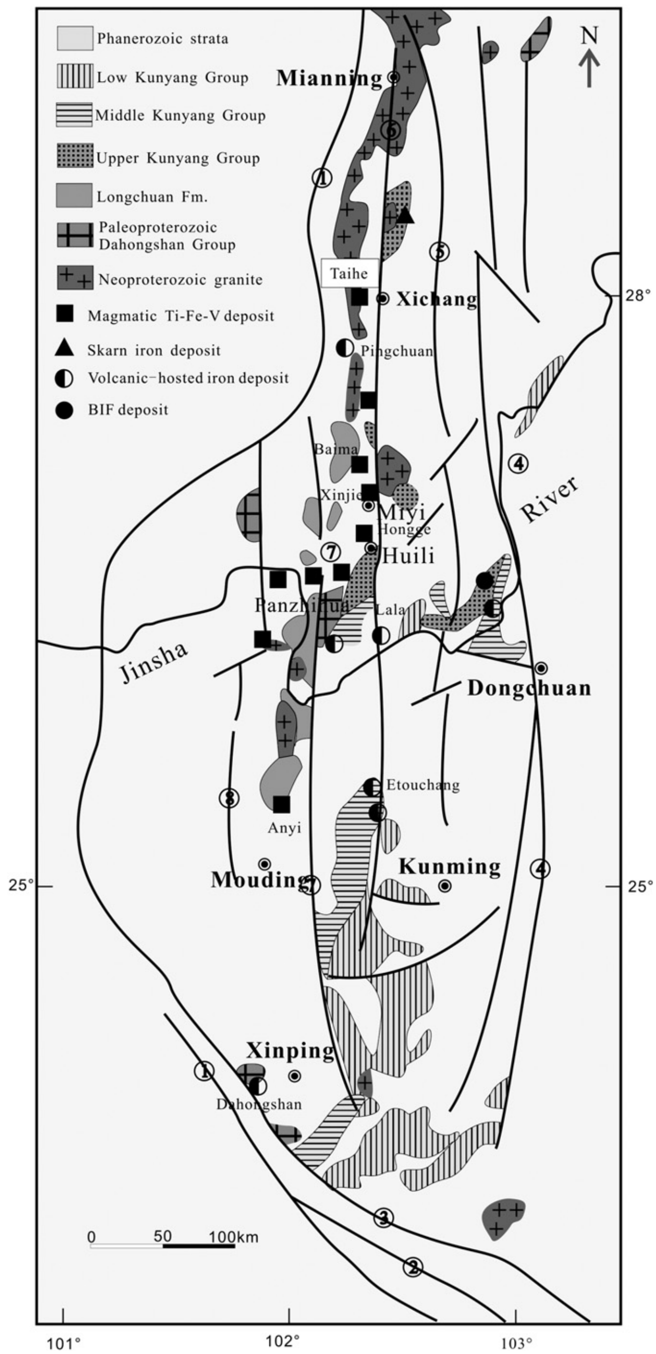

Fig. 5. Sketch geological map and distribution of the iron deposits from Xichang in Sichuan province to Xinping in Yunnan province. Fault number and name: ① Longmen–Ailaoshan fault; ② Ailaoshan fault; ③ Honghe fault; ④ Zhaojue–Xxiaojiang fault; ⑤ Heishanhe–Dianchi fault; ⑥ Anninghe–Yimen fault; ⑦ Yuanmou–Lüzhijiang fault; ⑧ Panzhihua–Chuxiong fault. Modified from Zhao et al. (2004).

Permian mafic and ultramafic intrusions are exposed along north–south-trending faults, and discontinuously form a 400-km-long belt from Mianning in the north, through Xichang, Miyi, and Panzhihua in Sichuan Province, to Mouding in Yunnan Province in the south (Fig. 4), which have been attributed to the Emeishan mantle plume (e.g., Hou et al., 2012, 2013; Zhang et al., 2009).

Four types of iron deposits namely magmatic Ti–Fe–(V) deposits, volcanic-hosted iron deposits, skarn iron deposits and BIFs have been recognized in the iron ore cluster (Fig. 4). However, magmatic Ti–Fe–(V) deposits are the most important iron resources, and the volcanic-hosted iron deposits are the second most important in the ore cluster.

The volcanic-hosted iron deposits are associated with the terminal Paleoproterozoic submarine basic volcano-sedimentary succession of the Dahongshan Group, Hekou Formation, Kunyang Group, which have undergone low-grade metamorphism such as the Dahongshan and Etouchang in Yunnan province and Lala in Sichuan province (Zhao, 2010). In these iron deposits, post-magmatic alteration such as albite and skarn alteration, is widespread. High-grade iron ores are dominant, but disseminated ores are also common, with no sharp boundaries with their country rocks. Magnetite is the dominant ore mineral. However, the ores also contain variable base metal sulfides, which formed later. In the Dahongshan iron deposits, the accompanying copper deposit is large in scale.

The magmatic Ti–Fe–(V) deposits are spatially and temporally associated with Middle Permian layered mafic–ultramafic intrusions, which have been dated by U–Pb zircon method at ~260 Ma (e.g., Hou et al., 2012, 2013; Zhou et al., 2005). These are associated with felsic intrusions, and are a part of ~260 Ma Emeishan large igneous province. Although these mafic–ultramafic intrusions occur along N–S-trending faults, they can be divided into the east and west belts. The east belt where Taihe, Baima and Hongge iron deposits occur is located in a narrow zone between Anninghe and Lüzhijiang faults (Fig. 5), and the west belt where Panzhihua and Anyi iron deposits occur is situated in the west side of the Lüzhijiang fault (Fig. 5).

In addition, the Pingchuan large high-grade iron deposit is associated with the Middle Permian picritic porphyry that intruded the Early Permian carbonate rocks overlain by the Middle Permian Emeishan flood basalts. However, unlike the contemporaneous Panzhihua iron deposit, the Pingchuan iron ores are characterized by low Ti and V as well as extensive calcite alteration, indicating hydrothermal origin (Wang et al., in this issue).

5.4. Middle–Lower Yangtze River Valley iron ore cluster

The Middle–Lower Yangtze River Valley (MLYRB) iron ore cluster is located along the northern margin of the SCB, extending for approximately 450 km from Daye (Hubei Province) in the west to Zhenjiang (Jiangsu Province) in the east (Fig. 6). It is also an important Cu–Au–Fe–S ore belt associated with Mesozoic magmatic rocks in SE China, and is characterized by skarn Fe deposits in the uplifted areas and apatite–magnetite deposits in Cretaceous down-faulted basins, with a total reserve of ~3.2 billion tons of iron ores, which accounts for ~5.9% of the total reserve of China.

The stratigraphic sequence in the ore cluster consists of three units: 1) Pre-Paleoproterozoic metamorphic basement, 2) Mesoproterozoic to Early Triassic submarine sedimentary cover and 3) Middle Triassic to Cretaceous terrigenous clastic and volcanic rocks. The basement rocks in the ore cluster include Paleoproterozoic to Archean amphibolite and granulite facies and supracrustal rocks, exhibiting pervasive migmatization (Chang et al., 1991; Zhai et al., 1992). The basement is overlain by a 2000-m-thick sequence of Meso- to Neoproterozoic volcano-sedimentary rocks that have been moderately metamorphosed to schists and gneisses. A recent biostratigraphic investigation has suggested that, starting in the Cambrian, thick (~1 km) carbonate and clastic sequences were deposited, and a large number of organic-rich black shales and chert nodules as well as phosphorous layers and nodules were formed in response to several anoxic events during the Paleozoic.

In the MLYRB, the Mesozoic magmatism developed in the Late Jurassic and Early Cretaceous. Three types of Mesozoic igneous rocks have been recognized: (1) A high-K calc-alkaline group, composed of diorite, quartz diorite, and granodiorite, which belong to the I-type (Pei and Hong, 1995). (2) A calc-alkaline group consisting of pyroxene dioritic porphyry, hornblende pyroxene dioritic porphyry, gabbro and eruptive correlatives. The volcanic rocks are exposed in five Late Mesozoic subaerial basins,

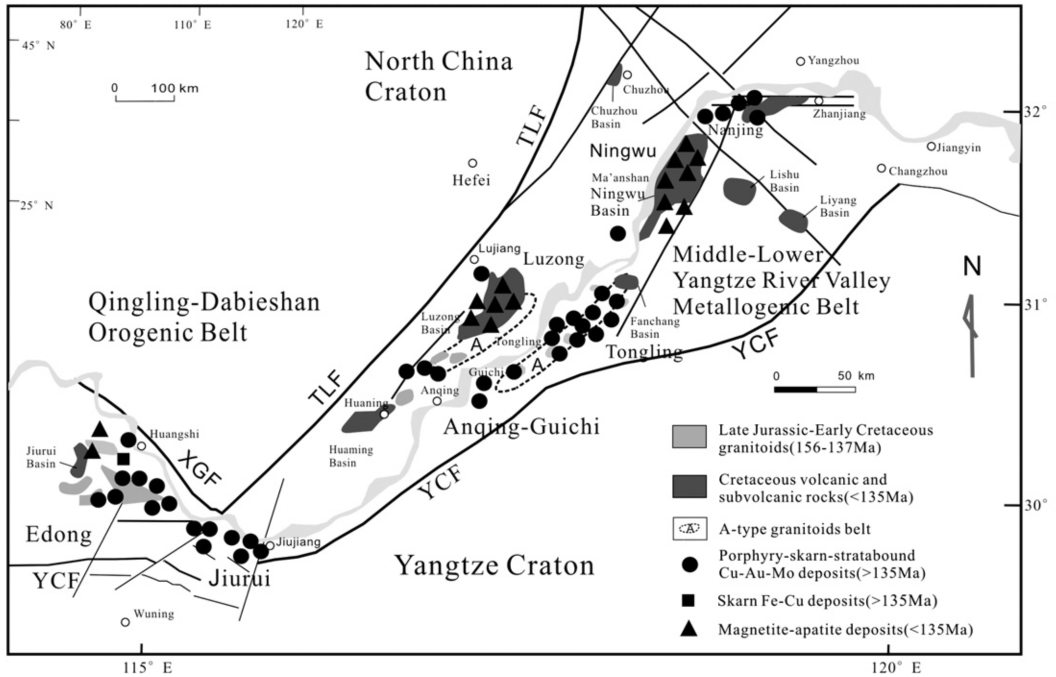

Fig. 6. Map showing the distribution of Fe–Cu deposits, related granitoids and Cretaceous basins along the Middle–Lower Yangtze River Valley metallogenic belt. TLF — Tancheng–Lujiang fault, XGF — Xiangfan–Guangji fault, YCF — Yangxing–Changzhou fault. Note: South China Block is traditionally considered to be composed of Yangtze Craton and Cathaysian Block. Modified from Mao et al. (2011).

which from west to east, are Jinbao–Huaining, Luzong, Fanchang and Ningwu basins, with a total area of about 5000 km^2 (Pan and Dong, 1999). These volcanic rocks have been dated at 127 to 135 Ma by zircon U–Pb methods (Fan et al., 2008; Yan et al., 2009; Zhou et al., 2008, 2010 and reference therein). (3) A-type granitoids consisting of quartz syenite, syenite, quartz monzonite, alkaline granite, and eruptive equivalents (rhyolite).

Extensive networks of faults and folds occur in the region. The numerous uplifts and down-faulted volcanic basins in the MLYRB were formed during the Triassic. The most extensive Middle Jurassic to Early Cretaceous NE–NNE-striking folds and faults, induced by the subduction of Pacific plate, overprinted previous deformation structures and formed several fault-controlled basins, such as the Ningwu and Luzong, which are filled with terrigenous clastic and volcanic rocks.

The iron deposits are of two types: apatite–magnetite deposits and skarn Fe deposits. They are related to calc-alkaline group (pyroxene dioritic porphyry, hornblende pyroxene dioritic porphyry) and high-K calc-alkaline group (diorite, quartz diorite, and granodiorite) respectively. The skarn Fe deposits occur only in the uplifted areas and controlled by intersections of EW- and NW-trending fractures. The iron orebodies occur at the contact between granitoids and Early Triassic carbonates intercalated with sandstone and shale. The recent LA–ICP–MS zircon U–Pb datings of ore-related granitoids have yielded ages of 134 to 127 Ma (Xie et al., 2008), identical to the mica Ar/Ar plateau ages of 132.6 ± 1.4 and 131.6 ± 1.2 Ma (Xie et al., 2008). In general, most massive ores were formed at the stage of retrograde alteration, and subsequently overprinted by pyrite-dominant mineralization. In contrast, the apatite–magnetite deposits are present in the Ningwu and Luzong Cretaceous terrigenous volcanic basins, which are controlled by NE- or NNE-striking faults. So far, there are 35 known apatite–magnetite deposits in the NNE-trending Ningwu basin and 11 known apatite–magnetite deposits in the NE-trending Luzong basin. The results from LA–ICP–MS U–Pb zircon dating indicate that the ore-related dioritic subvolcanic intrusions formed at 134–124 Ma (Fan et al., 2008; Hou et al., 2011, and reference therein), coeval or slightly later than those related to skarn Fe deposits. However, there are also some transitional ore systems between these two types of iron deposits, such as the Chengchao and Jinshandian Fe deposits in the Edong region in the northeast of the Jinniu Cretaceous basin (Mao et al., 2011).

5.5. Handan–Xingtai iron ore cluster

The Handan–Xingtai iron ore cluster is located in the southern Hebei Province, and is tectonically located in the transitional region between uplifted area and down-faulted basin in North China craton. There are 73 skarn Fe deposits in the ore cluster, with a total reserve of 830 Mt tons of iron ores.

The most extensive NNE- and SN-striking folds and faults overprinted previous EW-trending structures in the basement. The exposed strata include Cambrian–Ordovician sedimentary sequence and Carboniferous–Permian sedimentary sequence (Fig. 7). The Middle Ordovician Majiagou Formation, which is composed of thick-layer limestone intercalated with dolomitic limestone and marl with three anhydrite (evaporate) layers, is the main host rocks. The ore-related intrusions are Early Cretaceous diorite and monzonite with minor gabbro such as the Fushan, Xishimen, Guzhen, Beiminghe and Qicun intrusions. Recent zircon U–Pb analyses on these intrusions have yielded ages of ca. 130 Ma (Zheng et al., 2007a,b and reference therein), coeval with the Chengchao and Jinshandian iron deposits in the Daye area (Li et al., 2009) and apatite–magnetite deposits in MLYRV.

The iron orebodies occur at the contact between the Early Cretaceous dioritic intrusions and Middle Ordovician limestone or dolomitic limestone. From the contact zone profile, the shape of the ore bodies is reconstructed as complex lenses with end-to-end discontinuity. They are generally tens to hundreds of meters and up to 1000 m long, and tens to 100 m thick. The ore minerals are dominated by magnetite with minor hematite, pyrite, specularite, chalcopyrite, whereas the gangue minerals include diopside, tremolite, actinolite, phlogopite, serpentine, dolomite and calcite with minor chlorite, garnet and quartz. The ores have massive, disseminated, banded and breccia-like structures. Most of the ores are relatively high grade, with an average 40–60% Fe. In addition, they contain 0.07–2% S, 0.012–0.037% P and 0.013–0.1% Co, which are contained in pyrite.

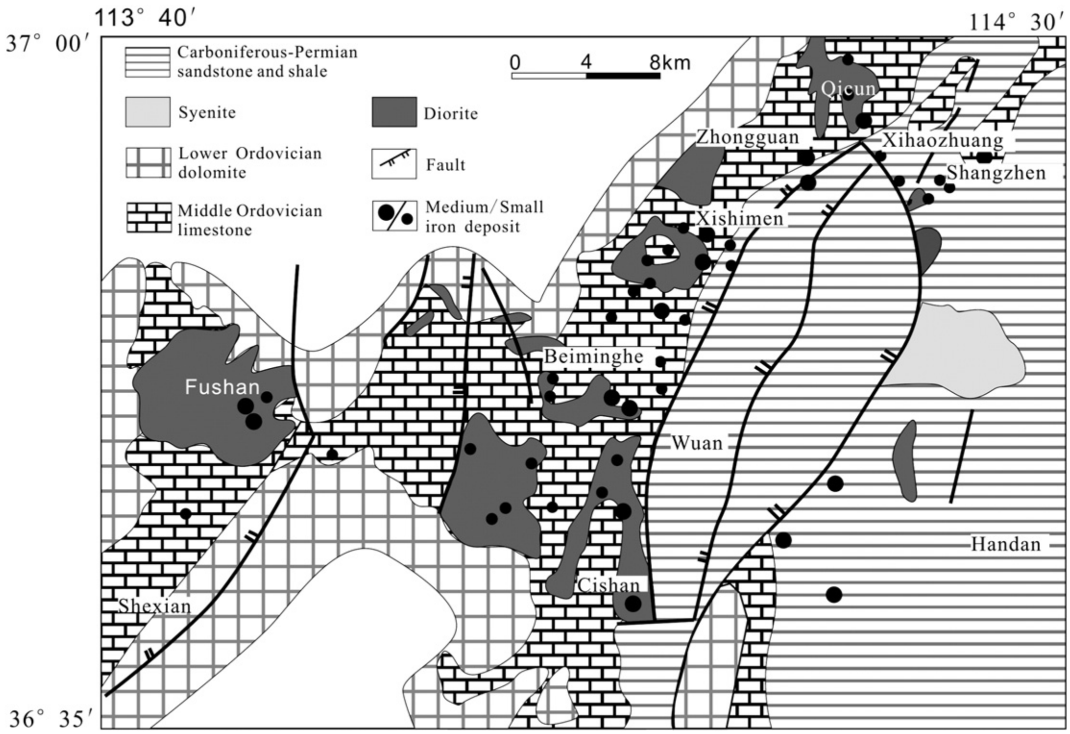

Fig. 7. Regional geological sketch map of the Handan–Xingtai iron ore cluster in Hebei province. Modified from Zheng et al. (2007b).

Alteration zones are clearly developed at the contact of the intrusive with the surrounding limestone. According to Zheng et al. (2007a), the mineralization and alteration processes can be divided into three stages: early albite and skarn alteration stage, middle retrograde alteration stage and late chlorite–carbonate–sulfide stage. Magnetite mineralization is closely associated with the middle retrograde alteration. In general, albite, scapolite and diopside alteration is very common, defining a distinct alteration zone within the dioritic intrusion. From the dioritic intrusion outward, the alteration zones can be divided into altered diorite zone (albite + scapolite + diopside + phlogopite + epidote ± prehnite), the endoskarn zone (diopside + garnet + phlogopite), the magnetite zone (50 to 80% magnetite, subhedral to anhedral grains from 0.15 to 0.4 mm in size), the exoskarn zone (diopside + tremolite + actinolite + serpentine) and the marble zone. In general, the endoskarn zone is wider than the exoskarn zone. The marble at the external contact zone has often been brecciated or altered by chlorite.

5.6. Awulale iron ore cluster

The Awulale iron ore cluster (Fig. 8), a part of Western Tianshan, is located along the southwestern margin of the Central Asia Orogenic belt (CAOB), a Neoproterozoic–Paleozoic orogenic belt extending from the Siberian Craton in the north to the Tarim Craton in the south (Windley et al., 2007; Xiao et al., 2004). In recent years, several large-medium iron deposits have been discovered or explored, such as Chagangnuoer, Beizhan, Zhibo, Dunde, Songhu, Wuling and Nixintage-Akesayi (Fig. 8). Thus, this is one of the most important iron ore clusters in China. All the iron deposits in the cluster are associated with submarine volcano-sedimentary successions, with a total reserve of ~1.17 billion tons of iron ores, among which about 30% of ores are of high grade (>50% Fe).

The Late Paleozoic tectonic evolution of the area can be broadly subdivided into two stages (e.g., Gao et al., 1998; Long et al., 2011): 1) Subduction-dominated, with the southward subduction of the North Tianshan Ocean or northward subduction of the South Tianshan Ocean beneath the Yili block, and north-directed A-type subduction of the Tarim Plate, followed by exhumation. 2) Post-collisional extension-dominated with a transition from subduction to post-collisional extension at ca. 320 Ma.

The exposed strata include Proterozoic, Silurian, Devonian, Carboniferous, Permian, Triassic, Jurassic and Quaternary. Among these, the Carboniferous and Silurian rocks are most widely distributed. Early Carboniferous and Early Permian volcanic rocks are well developed. The iron deposits are hosted in the Early Carboniferous volcanic-sedimentary sequences. They can be divided into two types, i.e., those hosted in lavas (e.g., Zhibo, Chagangnuuoer, Beizhan, Songhu, Dunde, Kuolasayi and Nixintage-Akesayi) and those hosted in volcanic clastic-sedimentary rocks (Shikebutai and Motuosala). In the first type, the ore-bearing volcanic rocks include basaltic, basalt-andesitic, andesitic and dacitic rocks. Magnetite is the dominant ore mineral although sulfides are common. Alteration is widespread, and K-feldspar, albite, epidosite, quartz and carbonate alteration is the most common. However, skarn alteration is also developed at the contact zone between the orebodies and carbonate rocks, which is different those of traditional skarns (with restricted occurrence at the contact zone between magmatic intrusion and Ca–Mg rich strata; e.g. Einaudi, 1981). However, magnetite formed at the stage of retrograde alteration. In the second type, the ore-bearing rocks include tuff and clastic rocks. The orebodies occur as stratiform and lentoid shape and display conformable contacts with the host rocks. The ore minerals consist predominantly of hematite with minor magnetite, and the gangue minerals are composed chiefly of chert and barite. Hematite is generally banded with red iron-bearing chert. In addition to iron, the ores contain some manganese minerals, e.g., blackmanganese and rhodochrosite. Spatially, the first type of iron deposits (e.g., Zhibo, Chagangnuuoer, Beizhan, and Dunde) is relatively close to the vent, whereas the second type of iron deposits (e.g., Shikebutai and Motuosala) is far from the vent, and the host rocks contain a large amount of re-sedimented epiclastic and pyroclastic debris.

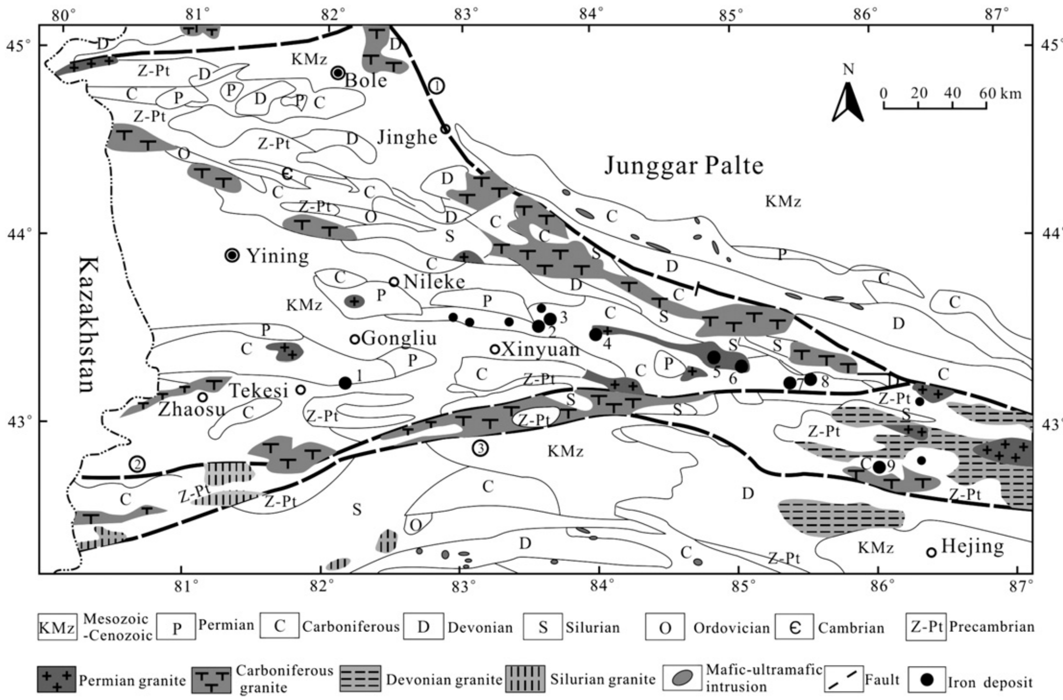

Fig. 8. Geological map of Western Tianshan Mountain and iron deposit. Awulale iron ore cluster is between 83°E and 86.5°E. Iron deposits: 1 — Kuolasayi; 2 — Shikebutai; 3 — Songhu; 4 — Nixintage–Aakesayi; 5 — Chagangnuoer; 6 — Zhibo; 7 — Dunde; 8 — Beizhan; 9 — Motuosala. Faults: ① — Yilianhabierga fault; ② — Nikolaev–North Nalati fault; ③ — Awuchangzi–Wuwamen fault.
After Z.H. Zhang et al. (2012).

6. Spatio-temporal evolution of the iron deposits in China

Despite a geological history dating back to the Paleoarchean, the oldest, well-recognized, economically significant iron deposits in China formed during Meso- and Neoarchean, especially at ~2.5 Ga (Shen, 1998; Shen et al., 2004), in contrast to the abundant Paleoproterozoic BIF deposits elsewhere in the world. All the BIF deposits formed in this period are distributed in the NCC. The generation of the ~2.5 Ga BIFs correlated to the accretion of microcontinental blocks to build the early tectonic architecture of the NCC (Santosh, 2010; Santosh and Kusky, 2009; Zhai and Santosh, 2011, 2013). During the process of the amalgamation, intense mafic-dominant tholeiitic magmatism is widespread in the NCC, and provided not only the source of iron, but also sufficient heat to drive the hydrothermal circulation, which is the critical factor for transportation and precipitation of iron. Hence, most of the BIF deposits at ca. 2.5 Ga are Algoma-type. The host strata include the Anshan Group in Anshan–Benxi area, Liaoning province, Luanxian and Zunhua Groups in eastern Hebei province, Sihetang Group in Miyun area, Beijing, Wutai Group in Shanxi province, Taishan Group in Shandong province, Dengfeng Group in Henan province and Huoqiu Group in Anhui province. These strata were formed in a continental margin.

Unlike in other cratons worldwide where the Paleoproterozoic marks major BIF deposition (James, 1983; Trendall, 2002), the BIF deposits formed during the Paleoproterozoic in China have only been recognized in the Lüliang Group, Shanxi province and Zhuzhangzi Group, eastern Hebei province. The formation of BIF deposits at this time was mainly related to rifts (or passive continental margins). The host rocks include a succession of metasedimentary sequence, and thus the BIF deposits can be classified into Superior-type. However, they account for only less than 25% of BIF deposits in China.

It is well known that the Early Precambrian atmosphere contained much lower oxygen levels than the Present (e.g., Basta et al., 2011; Morris, 1993; Walker et al., 1983; Young, 2013), so soluble iron is transported in the natural environments in the ferrous state. BIF deposition occurred through mixing of deep iron (and silica)-rich anoxic water with oxygenated surface seawater (e.g. Drever, 1974; Y.H. Li et al., 2012; Morris, 1993). The first great rise in atmospheric oxygen or the Great Oxidation Event (GOE) is generally thought to have occurred between ca. 2.45 and 2.2 Ga ago (e.g., Bekker and Kaufman, 2007; Bekker et al., 2004; Tang and Chen, 2013). However, Zhai and Santosh (2013) proposed that the global Great Oxidation Event left its imprint on the metallogenic systems in the NCC formed between ~2.35 and 2.0 Ga. The oxygenation of the atmosphere and the development of sufidic deep ocean by 1.8 Ga ago led to the cessation of BIF deposition (e.g., Canfield, 1998; Fairchild and Kennedy, 2007; Kump and Seyfried, 2005). Hence, no BIFs formed during this period (ca. 2.2 Ga to 1.8 Ga). It is noteworthy that the extensive mafic submarine volcanism occurred in an active continental margin along the southwestern margin of the SCB at ca. 1.9 Ga, and produced some volcanic-hosted iron deposits, e.g., Dahongshan and Etouchang deposits in Yunnan province and Lala deposit in Sichuan province. These iron deposits are hosted in the oldest unmetamorphosed submarine volcanic rocks so far as known.

During Mesoproterozoic (<ca. 1.8 Ga), the Chinese continents experienced breakup and aggregation. BIF deposits such as the Jingtieshan iron deposit in north Qilian mountains, Gansu province (Mao et al., 1999), formed in an extensional system were formed in the southwestern margin of the NCC,whereas V–Ti iron oxide deposits associated with Proterozoic anorthosite complex (e.g., Damiao in Chengde, Arndt, 2013a, 2013b; Li et al., in this issue) and "Xuanlong" type sedimentary hematite deposits formed in response to the Mesoproterozoic rift event in the NCC (Zhang et al., 2007; Zhao et al., 2009). In contrast, the iron deposits in some areas of the NCC and SCB occur in the active continental margin or island arc environment.

After a hiatus of over a billion years (from ca.1800 to ca. 800 Ma), BIFs re-appeared in the Neoproterozoic. Recent studies (e.g. Bekker et al., 2010; Ilyin, 2009) indicate the widespread distribution of Neoproterozoic iron formations, which embrace occurrences from all continents, which has been generally attributed to Snowball Earth (e.g., Hoffman et al., 1998; Klein and Beukes, 1993; Maruyama and Santosh, 2008). The BIF deposits are named Rapitan-type (e.g. Kirschvink, 1992). During the period of snowball Earth, the hydrosphere and oxygenated atmosphere were isolated by development of a thick ice cover, which led to the build-up of dissolved iron in the oceans through development of a more reduced hydrosphere (Basta et al., 2011). In contrast, Eyles and Januszczak (2004) attributed the reappearance of BIF in the Neoproterozoic to hydrothermal activity in embryonic rift basins accompanying the breakup of Rodinia. Comparably, many comparable BIF deposits have been reported from the SCB such as those of the Xinyu area, Jiangxi province and Qidong area in Hunan province. Although the precise age of the Shilu large high-grade iron deposits in Hainan province has not been well constrained, these BIFs were thought to have formed in the Neoproterozoic (e.g., Xu et al., 2013), and have been correlated to the global Snowball Earth as well as the imprint of the breakup of Rodinia by a superplume (e.g., Chu, 2004).

Subsequent to the Neoproterozoic Rodinian rifting of the Rodinia supercontinent, the three major cratons in China were existed as microcontinents throughout early Paleozoic (Li, 1998; Li et al., 1996). One of notable features is the "Ningxiang" type sedimentary hematite deposits that are widespread in the SCB during Early–Middle Devonian, Whereas active margins existed along both sides of the NCC, and the southern margin of the SCB, there is little evidence of significant oceanic plate subduction (Li, 1998). Late Paleozoic marks one of the most important episodes for the formation of two types of iron deposits, i.e., volcanic-hosted Fe deposits and magmatic Ti–Fe–(V) deposits. However, the two types of iron deposits formed in distinct tectonic settings. The volcanic-hosted iron deposits are mainly distributed in Central Asian Orogenic Belt (CAOB). They represent some of the later stages in a complex series of accretionary events that occurred for more than 200 million years between the Siberian craton and Tarim craton during the growth of Pangea (Cawood et al., 2009; Jahn et al., 2004; SengÖr and Natal'in, 1996), characterized by accretion of various terranes, such as ophiolites, accretionary prisms and possibly some microcontinents (Gao et al., 2011; Jahn et al., 2004; Xiao et al., 2009, 2010, 2013; Zheng et al., 2013). This period of Early Devonian to Carboniferous subduction–accretion was also associated with the widespread formation of volcanic-hosted iron deposits throughout these accreted terranes now exposed in northern Xinjiang, e.g., Mengku and Abagong in Altay (Chai et al., in this issue; Pirajno et al., 2011; Yang et al., 2010), and Beizhan, Zhibo and Chagangnuoer in western Tianshan (Duan et al., in this issue; Zhang et al., 2012c). The Early Permian extensional event following the Late Carboniferous collision led to post-collisional mafic magmatism in the East Tianshan and Beishan areas, which resulted in the formation of skarn iron deposits related to diabase such as the Cihai high-grade deposits in Xinjiang, and V–Ti iron oxide deposits associated with Cu–Ni sulfide deposits, e.g., Xiangshan, Niumaoquan and Haladala in Tianshan orogenic belt (Y.W. Wang et al., 2010). To the south of CAOB, extensive flood basaltic magmatism was widespread in the Tarim basin, forming Tarim large igneous province (TLIP), which has been attributed to mantle plume (Li et al., 2010; Mao et al., 2008; Pirajno et al., 2008; Zhang et al., 2010; Zhou et al., 2009). Some coeval mafic–ultramafic intrusions were emplaced in the northwestern TLIP. These intrusions host some of the medium–large V–Ti iron oxide deposits, e.g., Wajilitag and Puchang (Y.Q. Li et al., 2012; Zhang et al., in this issue). Slightly later, many ca. 260 Ma mafic and ultramafic intrusions were emplaced in the central Emeishan large igneous province, and they are exposed along north–south-striking faults, and discontinuously form a 400-km-long belt from Mianning in the north, through Xichang, Miyi, and Panzhihua in Sichuan Province, to Mouding in Yunnan Province in the south (Fig. 5). These rocks were produced by fractional crystallization of the parental Fe-rich picritic magma derived from partial melting induced by an upwelling mantle plume that involved an eclogite or pyroxenite component in the lithospheric mantle (Hou et al., 2011, 2013; Zhang et al., 2009).

The Triassic was characterized by collisions along many of the margins of the NCC, between the NCC and SCB, and the NCC and Siberian Craton (e.g. Ames et al., 1993; Li et al., 1993). Only minor skarn iron deposits and Ti–Fe–(V) deposits related to mafic intrusions formed following these collisions such as the Lizishan in Inner Mongolia and Cuihongshan in Heilongjiang province (Zhao et al., 2004), Weiya Ti–Fe–(V) deposits in East Tianshan, Xinjiang (236 ± 3 Ma, Wang et al., 2008).

The Yanshannian (Jurassic–Cretaceous) marks one of the most active periods of tectonomagmatism in Eastern China. Widespread intermediate-felsic intrusions were emplaced during this period, especially in Eastern China. Eastern China became an active continental margin at ca. 180 Ma (Maruyama et al., 1997; Qi, 1990) or before (Li and Li, 2007; Zhou and Li, 2000) since oblique subduction of the Izanagi plate beneath the Eurasian continent. The high-K calc-alkaline granitoid magmas were derived from melting of the subducted slab or metasomatised lithospheric mantle, with some input of crustal material (Li et al., 2009; Xie et al., 2008). These magmas were emplaced at the intersections between NE- and EW-trending faults and formed skarn Fe deposits between 146 and 127 Ma in the uplift areas along MLYRV (Li et al., 2009; Zhou et al., 2008, 2010). After 135 Ma the subducted plate changed its direction of motion to northeast, parallel to the Eurasian continental margin, and leading to large-scale back-arc-style extensional processes (Engebretson et al., 1985; Maruyama et al., 1997). The shoshonitic series and subsequent A-type granitoids magmatism and the development of apatite-bearing iron oxide deposits took place in both fault basins between 135 and 124 Ma in the Ningwu and Luzong basins in MLYRV. In the NCC, these geological entities have ages ranging from 135 to 115 Ma (Hu et al., 2008; Mao et al., 2008, 2011). Many large high-grade skarn iron deposits such as the Handan–Xingtai ore cluster in Central Hebei province and Zibo and Laiwu ore clusters in central Shandong province are associated with the ca. 130 Ma high-Mg dioritic rocks that were derived from an enriched lithospheric mantle, possibly contaminated by Ordovician evaporites during their emplacement. In recent years, some skarn iron deposits have been identified to be associated with granodiorite and monzogranite in the Gangdese belt, Tibet. The ore-hosted intrusions formed at ca. 113 Ma, which was considered to be induced by partial melting of the lithospheric mantle and the overlying crust in the back-arc extensional setting following southward subduction of the Bangonghu–Nujiang Ocean crust (Y.S. Yu et al., 2011).

In Cenozoic, most of the iron deposits were formed by weathering and leaching but they are medium to small in scale. Recently, some skarn iron deposits were discovered in the Gangdese belt, Tibet, although they have not been investigated in detail.

7. Summary

Although most of the major types of iron deposits reported worldwide have been recognized in China, the BIF, skarn, apatite–magnetite (low Ti), volcanic-hosted, sedimentary hematite and Ti–Fe–(V) deposits constitute the most economically important sources for iron. Among these, the skarn iron deposits are currently the major sources of high-grade iron ores in contrast to the scenario in Precambrian cratons elsewhere in the world where more than 85% high-grade iron ores are from BIF deposits. This difference can be attributed to the unique tectonic and geodynamic settings of China with the prolonged interaction of the Central-Asian, the Circum-Pacific and the Tethys–Himalaya systems. The oldest, well-recognized, and economically significant iron deposits in China are BIF deposits with a peak formation time at ~2.5 Ga. These deposits are mainly distributed in the NCC, and genetically correlated with the amalgamation of microcontinental fragments. Most of these deposits are Algoma-type associated with volcanic rocks. However, the BIF deposits formed during the Paleoproterozoic are Superior-type, but comprise only 25% of the BIF deposits in China, and are mainly related to rifts (or passive continental margins). During Meso-Neoproterozoic, some BIF deposits associated with sedimentary sequences were also formed in the southern and southwestern margin of the NCC and the SCB, whereas Ti–Fe–(V) deposits related to Mesoproterozoic anorthosite complex developed in the north margin of the NCC in response to rifting. Sedimentary hematite deposits formed in the NCC during Mesoproterozoic and in the SCB during Early–Middle Devonian occur in a shallow-marine environment.

Late Paleozoic marks one of the most important stages of formation of the volcanic-hosted iron deposits and magmatic Ti–Fe–(V) deposits. The iron deposits hosted in submarine volcanic sequences are mainly distributed in the CAOB, e.g., Altai and Tianshan, and are genetically related to a complex series of accretionary events during Devonian to Carboniferous. In southwestern China, many ca. 260 Ma mafic and ultramafic intrusions emplaced along north–south-striking faults in the central Emeishan large igneous province, generated the largest V–Ti–Fe ore cluster in the world.

The Yanshannian is the most important episode for skarn iron deposits and apatite–magnetite deposits. The large scale iron mineralization formed at ca. 130 Ma in an extensional setting. The skarn iron deposits are associated with calc-alkaline dioritic, granodioritic and granitic intrusions that were emplaced in the uplift areas in MLYRV and Central NCC. The apatite–magnetite deposits are concentrated in the NE-trending fault basins of the Ningwu and Luzong basins in MLYRV.

In Cenozoic, only minor medium–small skarn iron deposits formed, particularly those recently discovered in the Gangdese belt, Tibet.

Acknowledgments

We thank reviewers Profs. Jingwen Mao and Taofa Zhou for their thoughtful and constructive comments and suggestions. Financial support for this work was supported by Project 2012CB416806 of the State Key Fundamental Program (973), the National Natural Science Foundation of China (No. 40925006), Special Fund for Scientific Research in the Public Interest (200911007-25), the “Fundamental Research Funds for the Central Universities”, and the 111 Project (B07011). This work also contributes to the 1000 Talent Award to M. Santosh from the Chinese Government.

References

Ames, L., Tilton, G.R., Zhou, G.Z., 1993. Timing of collision of the Sino-Korean and Yangtse cratons: U–Pb zircon dating of coesite-bearing ecologites. Geology 21, 339–342.
Arndt, N., 2013a. The formation of massif anorthosite: petrology in reverse. Geosci. Front. 4, 195–198.
Arndt, N., 2013b. Intrusions of the Panxi region, China, and their magmatic ore deposits. Geosci. Front. 4, 479–480.
Basta, F.F., Mauriceb, A.E., Fontbotéc, L., Favargerd, P.Y., 2011. Petrology and geochemistry of the banded iron formation (BIF) of Wadi Karim and Um Anab, Eastern Desert, Egypt: Implications for the origin of Neoproterozoic BIF. Precambrian Res. 187, 277–292.
Bekker, A., Kaufman, A., 2007. Oxidative forcing of global climate change: a biogeochemical record across the oldest Paleoproterozoic ice age in North America. Earth Planet. Sci. Lett. 258, 486–499.
Bekker, A., Holland, H.D., Wang, P.L., Rumble III, D., Stein, H.J., Hannah, J.L., Coetzee, L.L., Beukes, N.J., 2004. Dating the rise of atmospheric oxygen. Nature 427, 117–120.
Bekker, A., Slack, J.F., Planavsky, N., Krapez, B., Hofmann, A., Konhauser, K.O., Rouxel, O.J., 2010. Iron formation: the sedimentary product of a complex interplay among mantle, tectonic, oceanic and biospheric processes. Econ. Geol. 105, 467–508.
Cai, B.J., Li, X.Z., Wei, S.P., Cui, Y.H., He, J.S., 1987. Features of the middle ordovician evaporites and its control over the endogenic iron (sulfur) deposits in Han-Xing district, Hebei. Bull. Inst. Geomech., CAGS No.10. 1–77 (in Chinese with English abstract).
Canfield, D.E., 1998. A new model for Proterozoic ocean chemistry. Nature 396, 450–453.
Cawood, P., Kroner, A., Collins, W., Kusky, T.M., Mooney, W.D., Windley, B.F., 2009. Earth accretionary orogens in space and time. Geol. Soc. Lond. Spec. Publ. 318, 1–36.
Chai, F.M., Geng, X.X., Yang, F.Q., Liu, F., Li, Q., Liu, G.R., 2013. The Abagong apatite-rich magnetite deposit in the Chinese Altay Orogenic Belt: a Kiruna-type iron deposit. Ore Geol. Rev. 57, 482–497 (in this issue).
Chang, Y.F., Liu, X.P., Wu, C.Y., 1991. The Copper–Iron Belt of the Lower and Middle Reaches of the Changjiang River. Geological Publishing House, Beijing 1–234 (in Chinese).
Chu, X.L., 2004. “Snowball Earth” during the Neoproterozoic. Bull. Mineral. Petrol. Geochem. 23, 233–238.
Dai, Y.P., Zhang, L.C., Wang, C.L., Liu, L., Cui, M.L., Zhu, M.T., Xiang, P., 2012. Genetic type, formation age and tectonic setting of the Waitoushan banded iron formation, Benxi, Liaoning Province. Acta Petrol. Sin. 28, 3574–3594 (in Chinese with English abstract).
Dill, H.G., 2010. The “chessboard” classification scheme of mineral deposits: mineralogy and geology from aluminum to zirconium. Earth Sci. Rev. 100, 1–420.
Dong, L.H., Feng, J., Zhuang, D.Z., Li, F.M., Qu, X., Liu, D.Q., Tang, Y.L., 2011. Discussion of metallogenic models, mineralization characteristic and main type of rich iron ore of Xinjiang. Xinjiang Geol. 29, 416–422 (in Chinese with English abstract).
Dong, H., Xing, C., Wang, C.Y., 2013. Textures and mineral compositions of the Xinjie layered intrusion, SW China: implications for the origin of magnetite and fractionation process of Fe–Ti-rich basaltic magmas. Geosci. Front. 4, 503–515.
Drever, J.I., 1974. Geochemical model for the origin of Precambrian banded iron formations. Geol. Soc. Am. Bull. 35, 1099–1106.
Duan, S.G., Zhang, Z.H., Jiang, Z.S., Zhao, J., Zhang, Y.P., Li, F.M., Tian, J.Q., 2013. Geology, geochemistry and age constraints on the Dunde iron–zinc deposit in Chinese western Tianshan. Ore Geol. Rev. 57, 441–461 (in this issue).
Einaudi, M.T., 1981. Skarn associated with porphyry plutons. I. Description of deposits, southwestern North America, II. General features and origin. In: Titley, S.R. (Ed.), Advances in Geology of the Porphyry Copper Deposits of Southwestern North America. University of Arizona Press, Tucson, pp. 139–183.
Engebretson, D.C., Cox, A., Gordon, E.G., 1985. Relative motions between the oceanic and continental plates in the Pacific basin. Geol. Soc. Am. Spec. Pap. 206, 1–56.
Eyles, N., Januszczak, N., 2004. 'Zipper-rift': a tectonic model for Neoproterozoic glaciations during the breakup of Rodinia after 750 Ma. Earth Sci. Rev. 65, 1–73.
Fairchild, I.J., Kennedy, M.J., 2007. Neoproterozoic glaciation in the Earth system. J. Geol. Soc. Lond. 164, 895–921.
Fan, Y., Zhou, T.F., Yuan, F., Qian, C.C., Lu, S.M., Cooke, D., 2008. LA–ICP–MS zircon U–Pb ages of the A-type granites in the Lu–Zong (Lujiang–Zongyang) area and their geological significances. Acta Petrol. Sin. 24, 1715–1724 (in Chinese with English abstract).
Gao, J., Li, M.S., Xiao, X.C., Tang, Y., He, G.Q., 1998. Paleozoic tectonic evolution of the Tianshan orogen, northwestern China. Tectonophysics 287, 213–231.
Gao, J., Klemd, R., Qian, Q., Zhang, X., Li, J.L., Jiang, T., Yang, Y.Q., 2011. The collision between the Yili and Tarim blocks of the Southwestern Altaids: geochemical and age constraints of a leucogranite dike crosscutting the HP–LT metamorphic belt in the Chinese Tianshan Orogen. Tectonophysics 499, 118–131.
Greentree, M.R., Li, Z.X., Li, X.H., Wu, H., 2006. Late Mesoproterozoic to earliest Neoproterozoic basin record of the Sibao orogenesis in western South China and relationship to the assembly of Rodinia. Precambrian Res. 151, 79–100.
Gross, G.A., 1965. Geology of iron deposits in Canada: general geology and evaluation of iron deposits. Geol. Surv. Can. Econ. Rep., 22, pp. 1–181.
Guo, P., Santosh, M., Li, S.R., 2013. Geodynamics of gold metallogeny in the Shandong Province, NE China: an integrated geological, geophysical and geochemical perspective. Gondwana Res. http://dx.doi.org/10.1016/j.gr.2013.02.004.
He, C., Li, S.Y., Gao, H.X., Wang, H.B., 2010. Geological condition of the Cuihonghsn skarn iron polymetalli deposits. Jilin Geol. 29 (3), 56–68 (in Chinese).
Hoffman, P.F., Kaufman, A.J., Halverson, G.P., Schrag, D.P., 1998. A Neoproterozoic snowball earth. Science 281, 1342–1346.
Hou, K.J., Li, Y.H., Wan, D.F., 2007. Constraints on the Archean atmospheric oxygen and sulfur cycle from mass-independent sulfur records from Anshan–Benxi BIFs, Liaoning Province, China. Sci. China D 50, 1471–1478.
Hou, T., Zhang, Z.C., Encarnacion, J., Du, Y.S., Zhao, Z.D., Liu, J.L., 2010. Geochemistry of Late Mesozoic dioritic porphyries associated with Kiruna-style and stratabound carbonate-hosted Zhonggu iron ores, Middle–Lower Yangtze Valley, Eastern China: constraints on petrogenesis and iron sources. Lithos 119, 330–344.
Hou, T., Zhang, Z.C., Kusky, T., 2011. Gushan magnetite–apatite deposit in the Ningwu basin, Lower Yangtze River Valley, SE China: hydrothermal or Kiruna-type? Ore Geol. Rev. 43, 333–346.
Hou, T., Zhang, Z.C., Encarnacion, J., Santosh, M., 2012. Petrogenesis and metallogenesis of the Taihe gabbroic intrusion associated with Fe–Ti-oxide ores in the Panxi district, Emeishan Large Igneous Province, southwest China. Ore Geol. Rev. 49, 109–127.
Hou, T., Zhang, Z.C., Pirajno, F., Santosh, M., Encarnacion, J., Liu, J.L., Zhao, Z.D., Zhang, L.J., 2013a. Geology, tectonic settings and iron ore metallogenesis associated with submarine volcanism in China: an overview. Ore Geol. Rev. 57, 498–517 (in this issue).
Hou, T., Zhang, Z.C., Encarnacion, J., Santosh, M., Sun, Y.L., 2013b. The role recycled oceanic crust in magmatism and metallogenesis: Os–Sr–Nd isotopes, U–Pb geochronology and geochemistry of picritic dykes in the Panzhihua giant Fe–Ti oxide deposit, central Emeishan large igneous province. Contrib. Mineral. Petrol. 165, 805–822.
Hu, R.Z., Bi, X.W., Zhou, M.F., Peng, J.T., Su, W.C., Liu, S., Qi, W.H., 2008. Uranium metallogenesis in South China and its relationship to crust extension during the Cretaceous to Tertiary. Econ. Geol. 103, 583–598.
Huang, K.J., Huang, K.Q., Li, J.L., 2006. The magmatism and its control to the skarn iron deposits in Tarshan area in southern Shanxi province. Geol. Res. 15, 205–211 (in Chinese with English abstract).
Ilyin, A.V., 2009. Neoproterozoic banded iron formations. Lithol. Miner. Resour. 44, 78–86.
Jahn, B.M., Auray, B., Coniicher, J., Bai, Y.L., Shen, Q.H., Liu, D.Y., 1987. 3.5 Ga old amphibolites from eastern Hebei province, China — field occurrence, petrography, Sm–Nd isochron age and REE geochemistry. Precambrian Res. 34, 311–346.
Jahn, B.M., Windley, B., Natal'in, B., Dobretsov, N., 2004. Phanerozoic continental growth in Central Asia. J. Asian Earth Sci. 23, 599–603.
James, H.L., 1983. Distribution of banded iron-formation in space and time. In: Trendall, A.F., Morris, R.C. (Eds.), Iron-Formation: Facts and Problems. Elsevier, Amsterdam, pp. 471–490.
Jiang, F.Z., 1983. A discussion on genetic types and metallogenic characteristics of the marine volcanic iron and/or copper deposits in China. Miner. Depos. 2, 11–18 (in Chinese with English abstract).
Jiang, F.Z., Wang, Y.W., 2005. Marine Volcanic Rocks and Related Metallic Ore Deposits. Metallurgical Industry Press, Beijing (in Chinese).
Kirschvink, J.L., 1992. Late Proterozoic low-latitude global glaciation: the snowball Earth. In: Schopf, J.W., Klein, C. (Eds.), The Proterozoic Biosphere: A Multidisciplinary Study. Cambridge University Press, pp. 51–52.
Klein, C., Beukes, N.J., 1993. Sedimentology and geochemistry of glaciogenic Late Proterozoic Rapitan iron-formation in Canada. Econ. Geol. 88, 542–565.

Konhauser, K.O., Amskold, L., Lalonde, S.V., Posth, N.R., 2007. Decoupling photochemical Fe(II) oxidation from shallow-water BIF deposition. Earth Planet. Sci. Lett. 258, 87–100.

Kump, L.R., Seyfried Jr., W.E., 2005. Hydrothermal Fe fluxes during the Precambrian: effect of low oceanic sulfate concentrations and low hydrostatic pressure on the composition of black smokers. Earth Planet. Sci. Lett. 235, 654–662.

Li, Z.X., 1998. Tectonic history of the major East Asian lithospheric blocks since the mid-Proterozoic: a synthesis. Mantle dynamics and plate interactions in East Asia. Geodynamics, 27, pp. 221–243.

Li, Z.X., Li, X.H., 2007. Formation of the 1300 km-wide intracontinental orogen and post-orogenic magmatic province in Mesozoic South China: a flat-slab subduction model. Geology 35, 179–182.

Li, S.G., Chen, Y., Cong, B.L., Zhang, Z., Zhang, R., Liou, D., Hart, S.R., Ge, N., 1993. Collision of the North China and Yangtze blocks and formation of coesite-bearing eclogites: timing and processes. Chem. Geol. 109, 70–89.

Li, Z.X., Zhang, L., Powell, C., 1996. Positions of the East Asian cratons in the Neoproterozoic supercontinent Rodinia. Aust. J. Earth Sci. 43, 593–604.

Li, J.W., Zhao, X.F., Zhou, M.F., Ma, C.Q., Souza, Z.S., Vasconcelos, P.M., Deng, X.D., Zhao, Y.X., Wu, G., 2009. Late Mesozoic magmatism from Daye region, Eastern China: U–Pb ages, petrogenesis and geodynamic implications. Contrib. Mineral. Petrol. 157, 383–409.

Li, Y.H., Hou, K.J., Wan, D.F., Zhang, Z.J., Yue, G.L., 2010. Formation mechanism of Precambrian banded iron formation and atmosphere and ocean during early stage of the earth. Acta Geol. Sin. 84, 1359–1373 (in Chinese with English abstract).

Li, H.M., Chen, Y.C., Li, L.X., Wang, D.H., 2012a. Metallogeny of the Iron Deposits in China. Geological Press, Beijing 1–246 (in Chinese).

Li, Y.H., Hou, K.J., Wan, D.F., Zhang, Z.J., 2012b. A compare geochemistry study for Algoma-and Superior-type banded iron formations. Acta Petrol. Sin. 28 (11), 3513–3519 (in Chinese with English abstract).

Li, Y.Q., Li, Z.L., Chen, H.L., Yang, S.F., Yu, X., 2012c. Mineral characteristics and metallogenesis of the Wajilitag layered mafic–ultramafic intrusion and associated Fe–Ti–V oxide deposit in the Tarim large igneous province, northwest China. J. Asian Earth Sci. 49, 161–174.

Li, H.M., Li, L.X., Zhang, Z.C., Santosh, M., Liu, M.J., Cui, Y.H., Yang, X.Q., Chen, J., Yao, T., 2013. Alteration of the Damiao anorthosite complex in the northern North China Craton: Implications for high-grade iron mineralization. Ore Geol. Rev. 57, 574–588 (in this issue).

Long, L.L., Gao, J., Klemd, R., Beier, C., Qian, Q., Zhang, X., Wang, J.B., Jiang, T., 2011. Geochemical and geochronological studies of granitoid rocks from the Western Tianshan Orogen: implications for continental growth in the southwestern Central Asian Orogenic Belt. Lithos 126, 321–340.

Ma, Y.X., Ji, X.T., Li, J.C., Huang, M., Min, Z.Z., 2003. Mineral resources of Panzhihua, Sichuan Province, SW China. Chengdu University of Technology, Chengdu (275 pp., in Chinese).

Mao, J.W., Zhang, X.Y., Zhang, Z.C., Ren, F.S., Zuo, G.C., Zhang, Z.H., Yang, J.M., Wang, Z.L., Ye, D.J., 1999. Temporal–spatial distribution and metallogenesis of polymetallic deposits in the western part of the Qilian. Acta Geol. Sin. 73, 230–241.

Mao, J.W., Wang, Y.T., Li, H.M., Pirajno, F., Zhang, C.Q., Wang, R.T., 2008. The relationship of mantle-derived fluids to gold metallogenesis in the Jiaodong Peninsula: evidence from D-O-C-S isotope systematics. Ore Geol. Rev. 33, 361–381.

Mao, J.W., Xie, G.Q., Duan, C., Pirajno, F., Ishiyama, D., Chen, Y.C., 2011. A tectono-genetic model for porphyry–skarn–stratabound Cu–Au–Mo–Fe and magnetite–apatite deposits along the Middle–Lower Yangtze River Valley, Eastern China. Ore Geol. Rev. 43, 294–314.

Maruyama, S., Santosh, M., 2008. Models on Snowball Earth and Cambrian explosion: a synopsis. Gondwana Res. 14, 22–32.

Maruyama, S., Isozaki, Y., Kimura, G., Terabayashi, M., 1997. Paleogeographic maps of the Japanese Islands: plate tectonic synthesis from 750 Ma to the present. Island Arc 6, 121–142.

Morris, R.C., 1993. Genetic modelling for banded iron-formation of Hamersley Group, Pilbara Craton, Western Australia. Precambrian Res. 60, 243–286.

Ningwu Research Group, 1978. Magnetite Porphyry Deposits in Ningwu Area. Geological Publishing House, Beijing 1–196 (in Chinese).

Nyström, J.O., Henriquez, F., 1994. Magmatic features of iron ores of the Kiruna type in Chile and Sweden: ore textures and magnetite geochemistry. Econ. Geol. 89, 820–839.

Pan, Y.M., Dong, P., 1999. The Lower Changjiang (Yangzi/Yangtze River) metallogenic belt, East China: intrusion- and wall rock-hosted Cu–Fe–Au, Mo, Zn, Pb, Ag deposits. Ore Geol. Rev. 15, 177–242.

Pang, K.N., Zhou, M.F., Qi, L., Chung, S.L., Chu, C.H., Lee, H.Y., 2013. Petrology and geochemistry at the Lower zone-Middle zone transition of the Panzhihua intrusion, SW China: Implications for differentiation and oxide ore genesis. Geosci. Front. 4, 517–533.

Pei, R.F., Hong, D.W., 1995. The granites of South China and their metallogeny. Episodes 18, 77–86.

Pickard, A.L., 2003. SHRIMP U–Pb zircon ages for the Palaeoproterozoic Kuruman Iron Formation, Northern Cape Province, South Africa: evidence for simultaneous BIF deposition on Kaapvaal and Pilbara Cratons. Precambrian Res. 125, 275–315.

Pirajno, F., Mao, J.W., Zhang, Z.C., Zhang, Z.H., Chai, F.M., 2008. The association of mafic–ultramafic intrusions and A-type magmatism in the Tian Shan and Altay orogens, NW China: Implications for geodynamic evolution and potential for the discovery of new ore deposits. J. Asian Earth Sci. 32, 165–183.

Pirajno, F., Seltmann, R., Yang, Y.Q., 2011. A review of mineral systems and associated tectonic settings of northern Xinjiang, NW China. Geosci. Front. 2, 157–185.

Qi, J.Z., 1990. Geodynamic background for Yanshanian endogenous metallogenesis in southern China. Bull. Nanjing Inst. Geol. Miner. Resour. Chinese Acad. Geol. Sci. 11, 1–15 (in Chinese with English abstract).

Qiao, G.S., Wang, K.Y., Guo, Q.F., Zhang, G.C., 1987. Sm–Nd dating of Caozhuang early Archean supracrustals, eastern Hebei. Chin. J. Geol. 1, 86–92 (in Chinese with English abstract).

Qiu, Y.M., Gao, S., McNaughton, N.J., Groves, D.I., Ling, W., 2000. First evidence of >3.2 Ga continental crust in the Yangtze Craton of south China and its implications for Archean crustal evolution and Phanerozoic tectonics. Geology 28, 11–14.

Ren, J.S., Wang, Z.X., Chen, B.W., 1999. See Tectonics of China from a Global Scale: A Brief Introduction to the Tectonic Map of China and Adjacent Areas. Geological Press, Beijing (33 pp., in Chinese).

Santosh, M., 2010. Assembling North China Craton within the Columbia supercontinent: the role of double-sided subduction. Precambrian Res. 178, 149–167.

Santosh, M., Kusky, T.M., 2009. Origin of paired high pressure–ultrahigh temperature orogens: a ridge subduction and slab window model. Terra Nova 22 (1), 35–42.

SengÖr, A.M.C., Natal'in, B.A., 1996. Paleotectonics of Asia — fragments of a synthesis. In: Yin, A., Harrison, M. (Eds.), The Tectonic Evolution of Asia. Cambridge University Press, Cambridge, pp. 486–640.

Shen, Q.H., 1998. Geology and Geological settings of the Early Precambrian banded iron formations in North China Craton. In: Cheng, Y.Q. (Ed.), Collections of Articles for in Geology of North China Craton in the Early Precambrian, pp. 1–30 (in Chinese).

Shen, B.F., 2012. Geological characteristics and resource prospect of the BIF type iron ore deposits in China. Acta Geol. Sin. 86, 1376–1395 (in Chinese with English abstract).

Shen, B.F., Yang, C.L., Zhai, A.M., Hu, X.D., 2004. Precambrian crustal evolution and mineralization in China. Miner. Depos. 23, 78–89 (Suppl., in Chinese with English abstract).

Song, X.Y., Qi, H.W., Hu, R.Z., Chen, L.M., Yu, S.Y., Zhang, J.F., 2013. Formation of thick stratiform Fe–Ti oxide layers in layered intrusion and frequent replenishment of fractionated mafic magma: evidence from the Panzhihua intrusion, SW China. Geochem. Geophys. Geosyst. 14, 712–732.

Sun, W.-H., Zhou, M.-F., Gao, J.-F., Yang, Y.-H., Zhao, X.-F., Zhao, J.-H., 2009. Detrital zircon U–Pb geochronological and Lu–Hf isotopic constraints on the Precambrian magmatic and crustal evolution of the western Yangtze Block, SW China. Precambrian Res. 172, 99–126.

Tang, H.S., Chen, Y.J., 2013. Global glaciations and atmospheric change at ca. 2.3 Ga. Geosci. Front 4, 583–596.

Tang, Y.C., Wu, C.Y., Chu, G.Z., Xing, F.M., Wang, Y.M., Cao, F.Y., Chang, Y.F., 1998. Geology of Copper–Gold Polymetallic Deposits in the along-Changjiang Area of Anhui Province. Geological Publishing House, Beijing (351 pp., in Chinese with English abstract).

Trendall, A.F., 2002. The significance of iron-formation in the Precambrian stratigraphic record. In: Altermann, W., Corcoran, P.L. (Eds.), Precambrian Sedimentary Environments: A Modern Approach to Depositional Systems. International Association of Sedimentologists Special Publication, 33, pp. 33–66.

Walker, J.C.G., Klein, C., Schidlowski, M., Schopf, J.W., Stevenson, D.J., Walter, M.R., 1983. Environmental evolution of the Archean–Early Proterozoic Earth. In: Schopf, J.W. (Ed.), Earth's Earliest Biosphere — Its Origin and Evolution. Princeton University Press, pp. 260–290.

Wan, Y.S., Liu, D.Y., Wang, S.J., Yang, E.X., Wang, W., Dong, C.Y., Zhou, H.Y., Du, L.L., Yang, Y.H., Diwu, C.R., 2011. 2.7Ga juvenile crust formation in the North China Craton (Taishan–Xintai area, western Shandong Province): Further evidence of an understated event from U–Pb dating and Hf isotopic composition of zircon. Precambrian Res. 186, 169–180.

Wang, Y.W., Wang, J.B., Wang, L.J., Long, L.L., 2008. Zircon U-Pb age, Sr-Nd isotope geochemistry and geological significance of the Weiya mafic-ultramafic complex. Xinjiang. Acta Petrol. Sinica. 24, 781–792.

Wang, Y.W., Wang, J.B., Wang, L.J., Long, L.L., Tang, P.Z., Liao, Z., Zhang, H.Q., 2010a. Petrological and lithogeochemical characteristics of the mafic–ultramafic complex related to CuNi–VTiFe composite mineralization: taking the North Xinjiang as an example. Acta Petrol. Sin. 26, 401–412 (in Chinese with English abstract).

Wang, W., Wang, S.J., Liu, D.Y., Li, P.Y., Dong, C.Y., Xie, H.Q., Ma, M.Z., Wan, Y.S., 2010b. Formation age of the Neoarchaean Jining Group (banded iron formation) in the western Shandong Province: constraints from SHRIMP zircon U–Pb dating. Acta Petrol. Sin. 26, 1175–1181 (in Chinese with English abstract).

Wang, Y., Fan, W., Zhang, G., Zhang, Y., 2013a. Phanerozoic tectonics of the South China Block: key observations and controversies. Gondwana Res. 23, 1273–1305.

Wang, M., Zhang, Z.C., Santosh, M., Hou, T., 2013b. Geochemistry of Late Permian picritic porphyries associated with Pingchuan iron ores, Emeishan Large Igneous Province, Southwest China: constraints on petrogenesis and iron sources. Ore Geol. Rev. 57, 602–617 (in this issue).

Windley, B.F., Alexeiev, D., Xiao, W., Kröner, A., Badarch, G., 2007. Tectonic models for accretion of the Central Asian Orogenic belt. J. Geol. Soc. London 164, 31–47.

Xiao, W.J., Windley, B.F., Badarch, G., Sun, S., Li, J.L., Qin, K.Z., Wang, Z.H., 2004. Palaeozoic accretionary and convergent tectonics of the southern Altaids: implications for the lateral growth of Central Asia. J. Geol. Soc. Lond. 161, 339–342.

Xiao, W.J., Kröner, A., Windley, B.F., 2009. Geodynamic evolution of Central Asia in the Paleozoic and Mesozoic. Int. J. Earth Sci. 98, 1185–1188.

Xiao, W.J., Huang, B.C., Han, C.M., Sun, S., Li, J.L., 2010. A review of the western part of the Altaids: a key to understanding the architecture of accretionary orogens. Gondwana Res. 18, 253–273.

Xiao, W.J., Windley, B.F., Allen, M.B., Han, C., 2013. Paleozoic multiple accretionary and collisional tectonics of the Chinese Tianshan orogenic collage. Gondwana Res. 23, 1316–1341.

Xie, G.Q., Mao, J.W., Li, L.R., Beirlein, F., 2008. Geochemistry and Nd–Sr isotopic studies of Late Mesozoic granitoids in the southeastern Hubei province, Middle–Lower Yangtze River belt, Eastern China: petrogenesis and tectonic setting. Lithos 104, 216–230.

Xu, D.R., Wang, Z.L., Cai, J.H., Wu, C.J., Bakun-Czubarow, N., Wang, L., Chen, H., Baker, M., Kusiak, A., 2013a. Geological characteristics and metallogenesis of the Shilu Fe-ore deposit in Hainan Province, South China. Ore Geol. Rev. 53, 318–342.

Xu, D.R., Wang, Z.L., Chen, H.Y., Wu, C.J., Jansen, N.H., Zhang, Z.C., Fu, W.W., 2013b. Petrography and geochemistry of the Shilu Fe–Co–Cu ore deposit, South China: implications for the origin of a Proterozoic BIF system. Ore Geol. Rev. 57, 322–350 (in this issue).

Yan, J., Liu, H.Q., Song, C.Z., Xu, X.S., An, Y.J., Liu, J., Dai, L.Q., 2009. Zircon U–Pb geochronology of the volcanic rocks from Fanchang–Ningwu volcanic basins in the Lower Yangtze region and its geological implications. China Sci. Bull. 54, 2895–2904.

Yang, F.Q., Mao, J.W., Liu, F., Chai, F.M., Guo, Z., Geng, X., Gao, J., 2010. Geochronology and geochemistry of the granites from the Mengku iron deposit, Altay Mountains, northwest China: implications for its tectonic setting and metallogenesis. Aust. J. Earth Sci. 57, 803–818.

Yang, Q.Y., Santosh, M., Shen, J.F., Li, S.R., 2013. Juvenile vs. recycled crust in NE China: Zircon U–Pb geochronology, Hf isotope and an integrated model for Mesozoic gold mineralization in the Jiaodong Peninsula. Gondwana Res. http://dx.doi.org/10.1016/j.gr.2013.06.003.

Young, G.M., 2013. Precambrian supercontinents, glaciations, atmospheric oxygenation, metazoan evolution and an impact that may have changed the second half of Earth history. Geosci. Front. 4, 247–261.

Yu, J.J., Chen, Y.C., Mao, J.W., Pirajno, F., Duan, C., 2011a. Review of geology, alteration and origin of iron oxide–apatite deposits in the Cretaceous Ningwu basin, Lower Yangtze River Valley, eastern China: implications for ore genesis and geodynamic setting. Ore Geol. Rev. 43, 170–181.

Yu, Y.S., Gao, Y., Yang, Z.S., Tian, S.H., Liu, Y.C., Cao, S.H., Hu, W.Z., Qie, H.M., 2011b. Zircon LA–ICP–MS U–Pb dating and geochemistry of intrusive rocks from Gunjiu iron deposit in the Nixiong ore field, Coqen, Tibet. Acta Petrol. Sin. 27 (7), 1949–1960.

Zhai, M.G., Santosh, M., 2011. The early Precambrian odyssey of the North China Craton: a synoptic overview. Gondwana Res. 20, 6–25.

Zhai, M.G., Santosh, M., 2013. Metallogeny of the North China Craton: Link with secular changes in the evolving Earth. Gondwana Res. 24, 275–297.

Zhai, Y.S., Yao, S.Z., Lin, X.D., Zhou, X.N., Wan, T.F., Jin, F.Q., Zhou, Z.G., 1992. Fe–Cu–Au Metallogeny of the Middle–Lower Changjiang Region. Geological Publishing House, Beijing 1–235 (in Chinese).

Zhai, Y.S., Xiong, Y.Y., Yao, S.Z., Liu, X.D., 1996. Metallogeny of copper and iron deposits in the Eastern Yangtze Craton, east–central China. Ore Geol. Rev. 11, 229–248.

Zhang, R.H., 1986. Sulfur isotopes and pyrite–anhydrite equilibria in a volcanic basin hydrothermal system of the Middle to Lower Yangtze River Valley. Econ. Geol. 81, 32–45.

Zhang, S.B., Zheng, Y.F., 2013. Formation and evolution of the Precambrian continental lithosphere in South China. Gondwana Res. 23, 1241–1260.

Zhang, S.H., Liu, S.W., Zhao, Y., Yang, J.H., Song, B., Liu, X.m, 2007. The 1.75–1.68 Ga anorthosite–mangerite–alkali granitoid–rapakivi granite suite from the northern North China Craton: Magmatism related to a Paleoproterozoic orogen. Precambrian Res. 155, 287–312.

Zhang, Z.C., Mao, J.W., Saunders, A.D., Ai, Y., Li, Y., Zhao, L., 2009. Petrogenetic modeling of three mafic–ultramafic layered intrusions in the Emeishan large igneous province, SW China, based on isotopic and bulk chemical constraints. Lithos 113, 369–392.

Zhang, C.L., Xu, Y.G., Li, Z.X., et al., 2010. Diverse Permian magmatism in the Tarim Block, NW China: Genetically linked to the Permian Tarim mantle plume? Lithos 119, 537–552.

Zhang, X.J., Zhang, L.C., Xiang, P., Wan, B., Pirajno, F., 2011. Zircon U–Pb age, Hf isotopes and geochemistry of Shuichang Algoma-type banded iron-formation, North China Craton: Constraints on the ore-forming age and tectonic setting. Gondwana Res. 20, 137–148.

Zhang, L.C., Zhai, M.G., Wan, Y.S., Guo, J.H., Dai, Y.P., Wang, C.L., Liu, L., 2012a. Study of the Precambrian BIF-iron deposits in the North China Craton: Progresses and questions. Acta Petrol. Sin. 28 (11), 3431–3445 (in Chinese with English abstract).

Zhang, L.C., Zhai, M.G., Zhang, X.J., Xiang, P., Dai, Y.P., Wang, C.L., Pirajno, F., 2012b. Formation age and tectonic setting of the Shirengou Neoarchean banded iron deposit in eastern Hebei Province: Constraints from geochemistry and SIMS zircon U–Pb dating. Precambrian Res. 222–223, 325–338.

Zhang, Z.H., Hong, W., Duan, S.G., Wang, Z.H., Li, M.W., Shi, F.P., Zhao, J., Zheng, R.Q., 2012c. Geological features, mineral ization types and metal logenic setting of Late Paleozoic iron deposits in western Tianshan Mountains of Xinjiang. Miner. Depos. 31, 941–964 (in Chinese with English abstract).

Zhang, D.Y., Zhang, Z.C., Huang, H., Encarnación, J., Zhou, N.W., Ding, X.X., 2013. Platinum–group elemental and Re–Os isotopic geochemistry of the Wajilitag and Puchang Fe–Ti–V oxide deposits, northwestern Tarim large igneous province. Ore Geol. Rev. 57, 589–601 (in this issue).

Zhao, X.F., 2010. Paleoproterozoic Crustal Evolution and Fe–Cu Metallogeny of the Western Yangtze block, SW China. (Ph.D. Thesis) The University of Hong Kong.

Zhao, G.C., Zhai, M.G., 2013. Lithotectonic elements of Precambrian basement in the North China Craton: review and tectonic implications. Gondwana Res. 23, 1207–1240.

Zhao, Y.M., Wu, L.S., Bai, G., Yuan, Z.X., Ye, Q.T., Huang, M.Z., Rui, Z.Y., Sheng, J.F., Lin, W.W., Deng, S.P., Mao, J.W., Bi, C.S., Dang, Z.F., Wang, L.F., Zhang, Z.H., Chen, W.S., 2004. Metallogeny of the Major Metallic Ore Deposits in China. Geological Press, Beijing (in Chinese).

Zhao, T.P., Chen, W., Zhou, M.F., 2009. Geochemical and Nd–Hf isotopic constraints on the origin of the 1.74–Ga Damiao anorthosite complex, North China Craton. Lithos 113, 673–690.

Zhao, H.J., Xie, G.Q., Wei, K.T., Ke, Y.F., 2012. Skarn mineral and stable isotopic characteristics of Tonglushan Cu–Fe deposit in Hubei Province. Geol. Rev. 58, 379–395 (in Chinese with English abstract).

Zheng, J.M., Mao, J.W., Chen, M.H., Li, G.D., Ban, C.Y., 2007a. Geological characteristics and metallogenic model of skarn iron deposits in the Handan–Xingtai area, southern Hebei, China. Geol. Bull. China 26 (2), 150–154 (in Chinese with English abstract).

Zheng, J.M., Xie, G.Q., Liu, J., Chen, M.J., Wang, S.M., Guo, S.F., Gao, X., Li, G.D., 2007b. Ar–Ar dating of phologopite from the Xishimen skarn iron deposits in the Handan–Xingtai area, southern Hebei, and its implications. Acta Petrol. Sin. 23, 2513–2518 (in Chinese with English abstract).

Zheng, C.N., Ouyang, Y.F., Wang, Y.Q., 2009. Geological characteristics and genesis of the Dading iron deposit in Guangdong Lianping. Gansu Metall. 31, 53–55 (in Chinese with English abstract).

Zheng, Y.F., Xiao, W.J., Zhao, G.C., 2013. Introduction to tectonics of China. Gondwana Res. 23, 1189–1206.

Zhong, H., Zhu, W.G., 2006. Geochronology of layered mafic intrusions from the Pan-Xi area in the Emeishan large igneous province, SW China. Miner. Deposita 41, 599–606.

Zhong, H., Yao, Y., Prevec, S.A., Wilson, A.H., Viljoena, M.J., Viljoena, M.P., Liu, B.G., Luo, Y.N., 2004. Trace-element and Sr–Nd isotope geochemistry of the PGE-bearing Xinjie layered intrusion in SW China. Chem. Geol. 203, 237–252.

Zhou, X.M., Li, W.X., 2000. Origin of Late Mesozoic igneous rocks in Southeastern China: implications for lithosphere subduction and underplating of mafic magmas. Tectonophysics 326, 269–287.

Zhou, M.F., Yan, D.P., Kennedy, A.K., Li, Y., Ding, J., 2002. SHRIMP U–Pb zircon geochronological and geochemical evidence for Neoproterozoic arcmagmatism along the western margin of the Yangtze Block, South China. Earth Planet. Sci. Lett. 196, 51–67.

Zhou, M.F., Robinson, P.T., Lesher, C.M., Keays, R.R., Zhang, C.J., Malpas, J., 2005. Geochemistry, petrogenesis and metallogenesis of the Panzhihua gabbroic layered intrusion and associated V–Ti–Fe oxide deposits, Sichuan Province, SW China. J. Petrol. 46, 2253–2280.

Zhou, T.F., Fan, Y., Yuan, F., Lu, S.M., Shang, S.G., Cooke, D., Meffre, S., Zhao, G.C., 2008. Geochronology of the volcanic rocks in the Luzong (Lujiang–Zongyang) basin and its significance. Sci. China D 51, 1470–1482.

Zhou, M.F., Zhao, J.H., Jiang, C.Y., 2009. OIB-like, heterogeneous mantle sources of Permian basaltic magmatism in the western Tarim Basin, NW China: Implications for a possible Permian large igneous province. Lithos 113, 583–594.

Zhou, T.F., Fan, Y., Yuan, F., Song, C.Z., Zhang, L.J., Qian, C.C., Lu, S.M., Cooke, D., 2010. Temporal–spatial framework of magmatic intrusions in Luzong volcanic basin in East China and their constrain to mineralization. Acta Petrol. Sin. 26, 2694–2714 (in Chinese with English abstract).

Zhou, T.F., Fan, Y., Yuan, F., Zhang, L.J., Ma, L., Qian, B., Xie, J., 2011. Petrogensis and Metallogeny study of the volcanic basins in the Middle and Lower Yangtze metallogenic belt. Acta Geol. Sin. 85, 712–730 (in Chinese with Englisj abstract).